UNIVERSITI
MALAYSIA
KELANTAN

PREPARATION AND SCREENING OF CROSS-LINKED MAGNETIC BIOCARBON FOR METHYLENE BLUE REMOVAL

GAN SUTENG
F15A0045

A thesis submitted to fulfil as a part of Bachelor of Applied Science (Product Development Technology) with Honours

FACULTY AGRO BASED INDUSTRY

2018

DECLARATION

I hereby declare that the work embodied in this report is the result of the original research and has not been submitted for a higher degree to any universities or institutions.

_____

Student

Name: GAN SUTENG

Date: 18/12/2018

I certify that the report of this final year project entitled "Preparation and Screening of Cross-Linked Magnetic Biocarbon for Methylene Blue Removal" by Gan SuTeng, matric number F15A0045 has been examined and all the correction recommended by examiners have been done for the degree of Bachelor of Applied Science (Product Development Technology) with Honours, Faculty of Agro-Based Industry, University Malaysia Kelantan.

Approved by:

_____

Supervisor Name: Prof. Palsan Sannasi Bin Abudullah

Date:

ACKNOWLEDGEMENT

Thanksgiving to the most gracious and merciful, God for the strengths and blessing for me in accomplishing this research. Secondly, I appreciated sincerely to my beloved family and Lean Choon Poh for their encouragements as well as moral and spiritual supports.

For academic institute, I would like to thank University Malaysia Kelantan (UMK), Faculty Agro Based Industry (FIAT) for providing high standard of education and experimental equipment. Throughout the project, it exposed me to real practical in lab work and scientific research. Sincere thanks to my great Final Year Project supervisor, Prof. Madya Dr. Palsan Sannasi Bin Abdullah for his impeccable guidance, continuous support, forgiving and useful critique throughout the experiments and thesis works. Besides, my academic advisor, Dr. Noor Hafizoh Binti Saidan was always aiding me in term of academy.

Throughout the FYP, I would like to express my sincere gratitude to lecturers for their help and endless motivational advices such as Dr. Leony Tham Yew Seng, Dr. Ikarastika, Dr. Khomaizon, and others. Meanwhile, lab staffs played important roles in accessing to equipment, materials and apparatus that required in lab work. Thousand thanks to lab assistants especially Madam Hidayah, Mr. Suhami, Mr. Rohanif, Mr. Qamal, Mr. Khaliq, Mr. Rohimi, Mr. Nik, and others. Special thanks to my FYP teammates Chan Ke Xin and Irene Tan Jia Lin, my friends like Low Siah Von, Loh Chek Swee, Lee Shall Ting, and others. Sincerely thanks to all the people who had help me along the FYP especially the people that I mentioned above.

Finally, I finished the FYP completely and successfully. Thanks you very much!

TABLE OF CONTENTS

LIST OF TABLES

LIST OF FIGURES

LIST OF SYMBOL

C_i	Initial concentration
C_f	Final concentration
cm	centimetre
g	gram
M	Molarity
mg/g	Milligram per gram
mg/L	Milligram per litre
R^2	Correlation Coefficient
rpm	Revolutions per minute
T_1	Treatment 1, MAC
T_2	Treatment 2, MAC-CTAB
T_3	Treatment 3, MAC-CPS
γ	Gamma
°	Degree
℃	Degree Celsius
Θ	Theta
Å	Angstrom
λ	Lambda
μm	Micrometre
%	Percentage

LIST OF ABBREVIATION

AC	Activated BioCarbon
CTAB	Cetyltrimethylammonium Bromide
CPS	Cyclopentasiloxane
C-C	Aromatic Functional Group
C=O	Carbonyl Functional Group
FTIR	Fourier transform infrared spectroscopy
Fe-O	Iron Oxide
Fe_3O_4	Magnetite
γ-Fe_2O_3	Maghemite
MAC	Magnetic Activated BioCarbon
MB	Methylene Blue
O-H	Alcohol/ Phenol Functional Group
pMAC	Provided Magnetic Activated BioCarbon
R-squared	Correlation Coefficient
SEM-EDS	Scanning Electron Microscope equipped Energy-Dispersive Spectroscopy
TGA	Thermogravimetric Analysis
XRD	X-ray diffraction

Pengolahan dan Penyaringan Biokarbon Magnetik yang Bersilang untuk Menyingkir Metilena Biru

ABSTRAK

Biokarbon Aktif Magnetik (MAC) bersilang dengan Cetyltrimethylammonium Bromida (CTAB) dan Cyclopentasiloxane (CPS) direka untuk menyingkirkan Metilena Biru (MB) dalam larutan air. MAC yang bersilang menunjukkan kemagnetan yang kuat untuk menjerapkan MB ke dalam MAC telah diskrin dan dikaji. Keberkesanan penyingkiran juga dibandingkan dengan MAC (T_1) yang tidak bersilang, biokarbon aktif (AC) (kawalan positif), dan MAC yang disediakan (pMAC) (kawalan negative). Ujian iodin, spektroskopi inframerahtransformasi Fourier (FTIR), X-ray pembelauan (XRD), mikroskop elektron pengimbas dilengkapi dengan tenaga serakan spektroskopi (SEM-EDS), dan analisis Termogravimetri (TGA) dijalankan bagi mengenal-pasti sifat-sifat fizikal dan kimia daripada sampel. MAC tersilang dengan CPS (MAC-CPS) menunjukkan kecekapan tertinggi di penyingkiran MB 99.84% dalam 60 min berbanding dengan CTAB bersilang(MAC-CTAB). Walau bagaimanapun, nomber iodin bagi MAC-CPS mencatatkan bacaan terendah dengan nilai 90.18 mg/g berbanding AC dan MAC. FTIR spektrum untuk MAC-CPS telah mendedahkan bahawa Si-O regangan dan Fe-O regangan dijumpai di 1254 cm^{-1} dan 525 cm^{-1} boleh berkaitkan kepada interaksi antara oksida besi dan CPS dalam reaksi silang. Analisis XRD memaparkan bahawa magnet fasa yang dihasilkan ialah magnetit (Fe_3O_4) dengan jumlah yang kecil maghemite (γ-Fe_2O_3). TGA menunjukkan MAC-CPS memiliki kestabilan haba yang lebih tinggi. Kesimpulannya, CPS berpotensi sebagai ejen bersilang untuk ujian praktikal selanjutnya.

Kata Kunci: Biokarbon Aktif Magnetik, Reaksi Silang, CTAB, CPS, Penyingkiran Metilena Biru

Preparation and Screening of Cross-Linked Magnetic Biocarbon for Methylene Blue Removal

ABSTRACT

A cross-linked iron oxide particle with activated biocarbon (MAC) by Cetyltrimethylammonium Bromide (CTAB) and Cyclopentasiloxane (CPS) was designed for the uptake of Methylene Blue (MB) in water solution. The cross-linked MAC was successfully prepared with strong magnetization property. The effect of contact time of MB onto newly prepared MAC samples was screened and studied. The removal effectiveness also compared with MAC (T_1), AC (positive control), and provided MAC (pMAC) (negative control). The physical and chemical properties of studied samples were obtained through iodine test, Fourier transform infrared spectroscopy (FTIR), X-ray diffraction (XRD), scanning electron microscope equipped with energy-dispersive spectroscopy (SEM-EDS), and thermogravimetric analysis (TGA). MAC cross-linked with CPS (MAC-CPS) showed highest efficiency in MB removal of 99.84 % in 60 min relative to CTAB cross-linking agent (MAC-CTAB). However, low iodine number obtained in MAC-CPS as 90.18 mg/g decreased compared to AC and MAC as 1007.01 mg/g and 240.48 mg/g respectively. The FTIR spectrum of MAC-CPS indicated intense of Si-O stretching and Fe-O stretching at 1254 cm^{-1} and 525 cm^{-1} respectively. This can be assigned to the interaction between iron oxide and CPS in cross-linked reaction. The analysis of XRD suggested that the main magnetic phase present is magnetite (Fe_3O_4) with small amounts of maghemite (γ-Fe_2O_3). The TGA demonstrates MAC-CPS possessed higher thermal stability property. The excellent characteristics presented by CPS potential as cross-linking agent for further practical applications.

Keywords: Magnetic Activated Biocarbon, Cross-linked, CTAB, CPS, Methylene Blue Removal.

CHAPTER 1

INTRODUCTION

1.1 Research Background

In the last few decades, environmental pollution due to indiscrimination disposal of toxic and even carcinogenic inorganic dyes from related industries such as paper, plastic, leather, and textile generating coloured wastewater and increasing worldwide concern. Dyes are known as not biodegradable not only lead to adverse environmental effects but also threaten to aquatic organisms as it limited the light penetration for photosynthesis despite they are present at low concentrations. Moreover, it is recognized that public perception of water quality is depending on colour performed. The colour is the first contaminant to be discriminated in wastewater (Rafatullah, Sulaiman, Hashim, & Ahmad, 2010). As a result, an environmental friendly and cost-effective treatment is highly required to remove them from wastewater before being discharged into the environment.

Biocarbon, a porous and carbon-rich residue created through the thermal conversion of biomass or biological residues including wood residues (Sivakumar, Kannan, & Karthikeyan, 2012), biomass waste (Cazetta et al., 2011), food residues, and etc under anaerobic conditions has encouraged a growing exploration in production. A bulk of research was found focused on the application of biocarbon as sustainable adsorbents (Gwenzi, Chaukura, Noubactep, & Mukome, 2017), bioenergy (Laird, 2008) and soil amendment (Beesley et al., 2011) due to high efficient, cost effective and environmental-friendly properties. Mohan, Sarswat, Ok, & Pittman (2014) demonstrated that biocarbon may be introduced as a modifier or carbon sink to eliminate the emission of greenhouse CO_2 from decaying biomass.

Several researches have been carried out to determine the used modified bio-char as adsorbent in water treatment applications to remove various pollutants, including heavy metals (Dias, Alvim-Ferraz, Almeida, Rivera-Utrilla, & Sánchez-Polo, 2007), inorganic and organic compounds (Inyang, & Dickenson, 2015) and microbial contaminants (Zimmerman, Gao, & Ahn, 2011). Gwenzi, Chaukura, Noubactep, & Mukome (2017) demonstrated that "compared to existing low-cost water treatment techniques, biocarbon technology provides multiple environmental and agronomic co-benefits, making it attractive in developing countries". The shortcoming of biocarbon is notoriously difficult of its separation from the solution thus resulting time-consuming and increasing operation cost. Therefore, there is a need to develop a technique to collect them from aqueous solutions to avoid secondary pollution.

The composites of carbon and microcrystals of ferromagnetic materials have received much attention of scientists to develop a potential novel adsorbent that provided with adsorptive and magnetic dual functionalities (Zhou et al., 2014). The main interest of this technology consists in its capability of treating large amount of wastewater within

a short time with contaminants free environment (Gong et al., 2009). There were numerous researches published on the cross-linked of magnetic chitosan with epichlorohydrin (Sharma et al., 2014), ethylenediamine (Hu et al., 2011), and glutaraldehyde (Donia, Atia, & Elwakeel, 2008) to improve the removal of organic or inorganic compounds from aqueous solution. Luo & Zhang (2009) also have reported that the magnetic cellulose beads entrapping activated carbon with epichlorohydrin could efficiency adsorb organic dyes. In the literature, however, studies about cross-link iron oxide particle with activated biocarbon (AC) by cross cetyltrimethylammonium bromide (CTAB) and cyclopentasiloxane (CPS) have less or never been reported. Therefore, methylene blue was selected as model dye to analyse the removal effect by of iron impregnated AC (MAC). The decolourization of methylene blue was chosen as prior indicator of technology effectiveness.

1.2 Problem Statement

The large amount of coloured wastewater release due to the accelerate of textile industries in Malaysia has attracted concern of environmentalists in the last few years. Ben Mansour et al. (2012) demonstrated that "the wastewater from textile plants is classified as the most polluting of all the industrial sectors, considering the volume generated as well as the effluent composition". Moreover, the complex aromatic molecular structures and complex structure of dyes make them more stable and more resistance to decompose by treatment (Robinson et al., 2001). Thus, coloured wastewater poses a challenge to the conventional wastewater treatment techniques.

Some of commercial adsorbents that used for dye effluent application are high cost as precursor derived from non-renewable source or expensive precursor material such as coal and coke (Chakraborty, DasGupta, & Basu, 2005). On the other hand, agricultural wastes including nut shells, rice husk, oil palm kernel, coconut shell, and etc are reported the most abundant biomass that being disposed in Malaysia due to the wastes is considered as non-valuable or else caused by poor management of disposal material (Yusof, Yahya, & Adam, 2015). The poor management in agricultural wastes was eventually cause adverse effect on the living microorganisms as well as creates significant environmental degradation.

Biocarbon based adsorbents is well-known as adsorbent or precursor material for production of AC due to their excellent proximate analysis including low ash and moisture content that presented by several researches (Robinson, McMullan, Marchant, & Nigam, 2001). The major drawback of the AC is related to difficult separation from the treated water. This not only limited its application in large-scale applications somehow caused a secondary pollution in certain situation (Strachowski, Kaszuwara, & Bystrzejewski, 2017).

1.3 Objectives

1. To prepare MAC cross-link with CTAB and CPS.
2. To screen the adsorption effectiveness of the newly prepared MAC for the uptake of methylene blue dye.
3. To characterize the physical and chemical properties of the newly prepared MAC.

1.4 Scope of Research

In this present work, MAC cross-linked with the CTAB (MAC-CTAB) and CPS (MAC-CPS) were prepared to improve the adsorption capacity of organic dyes. Methylene Blue (MB) was selected as model dye to investigate and screen the adsorption performance and adsorption capacity of MAC-CTAB, and MAC-CPS under laboratory conditions. The removal effectiveness also compared with MAC, AC (positive control) and provided MAC (pMAC) (negative control).

Characterization of MAC, MAC-CTAB, and MAC-CPS were conducted to evaluate the physical and chemical properties via iodine test, Fourier transform infrared spectroscopy (FTIR), X-ray diffraction (XRD), scanning electron microscopy equipped with energy-dispersive spectroscopy (SEM-EDS), thermogravimetric analysis (TGA).

1.5 Significance of Research

Environmental issues of dye pollution caused by textile industries has been reported in many Malaysia. Thus finding of this study can be beneficial in removing dyes and enhancing environment to a quality standard. The application of magnetic loaded biocarbon designing a low cost and more easily recovered or manipulated alternative solution in wastewater treatment due to its excellent performance in adsorption of dyes and high separation efficiency. Last but not least, there are many dye removal researches have been done by using magnetic carbon cross-linked with epichlorohydrin and glutaraldehyde but less detailed studies available regarding the use of CTAB and CPS as cross linker. Therefore, the information gained in this study may help in improving

knowledge regarding the adsorption efficiency of MAC with cross linker in colour removal from dye-containing effluents.

1.6 Limitation of Research

There is limited resources and equipment available in university. The insufficient of machine provided delay the lab work progress. In order to save time, some equipment is needed to share among researchers who were same parameter used. However, the unknown chemical contained inside caused contamination with sharing material and contributed an inaccurate or unexpected outcome of the research result.

CHAPTER 2

LITERATURE REVIEW

2.1 Dye Pollution

Dyes are natural or synthetic substance that capability impart colour to surfaces or fabrics. In twentieth century, synthetic dyes practically replaced natural compounds due to its complex molecular structure which makes them stable and more resistant to the action of detergents, light, soap solution, and water (Gupta, Mittal, Kurup, & Mittal, 2006). However, it is recognized to be one of the heavy contaminations of water bodies, due to the large consumption of colourings needed in clothing, food, personal care products, paper, paints and plastics. At least 25% of the world population are suffering from coloured effluent that discharged into water bodies (Soon & Hameed, 2011).

Textile industry, the main income source in many developing countries has been identified as one of the significant industries that contributed to environmental dye pollution (Robinson, McMullan, Marchant, & Nigam, 2011). Large quantities of chemicals and water is utilised during the production process. Kallel et al. (2016)

demonstrated that the annual production of dyes over 7×10^5 tonnes/year. The total dye consumption in the textile industry worldwide is more than 10,000 tonnes/year and approximately 5 - 10 % tonnes/year of dyestuffs is discharged into water streams.

The water that used for application of dyes onto the fibres contains large amount of poisonous and dangerous chemicals including zinc, arsenic, lead, copper, mercury, and certain auxiliary chemicals. The high recalcitrant dyes not only mutagenic and toxic to humans also brings negative impact to environment. For example, textile waste water can cause ulceration of skin, haemorrhage, skin irritation, eye irritation, and dermatitis (Tsai, Hsien, & Hsu, 2009). While the undesirable chemicals discharged into water reduce the penetration of sunlight and inhibiting photosynthesis of aquatic plants thereby effect the aquatic food web (Wong, Yac'cob, Ngadi, Hassan, & Inuwa, 2018). In addition, Oz, Lorke, Hasan, & Petroianu (2010) illustrated that "the safety of seafood is compromised due to biomagnification and bioaccumulation effects of dyes molecules in the marine ecosystem. Transfer of these compounds into human body though ingestion of seafood could lead to undesirable and irreversible effects to human nervous systems".

2.2 Methylene Blue (MB) Dye

A cationic thiazine dye, MB with IUPAC name 3,7-bis(Dimethylamino)-phenothiazin-5-ium chloride have molecular formula $C_{16}H_{18}N_3SCl$ and the molecular weight of 319.85 g mol^{-1}. It shows deep blue colour in oxidized state but colourless in reduced form, leukomethylene blue (LMB) (Cragan, 1999). MB is a common soluble dye found in water, in widely used for calico, printing, medicinal purposes, and tannin (Gupta

et al., 2004). It also been general used as model of dye in textile industry due to its intense blue appearance.

MB is water soluble where it dissociates into anion. MB also can lead to salt formation and develop the colour fade upon fabrics due to the electrostatic attraction build up between the coloured cation and acidic groups of acrylic fibres. MB structure is shown in Figure 2.1.

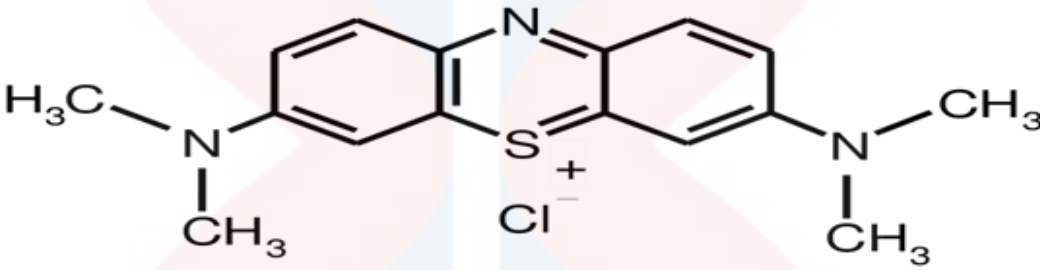

Figure 2.1: The molecular structure of methylene blue.

Source: Cragan (1999).

It has been reported that approximately 5–20 % of MB dyes are discharged into water bodies annually (Teow, Nordin, & Mohammad, 2018). The non-biodegradability property causes a disastrous influence to the aquatic ecosystem. The coloured effluent polluted the environment by inhibiting the penetration of light into the water source and depleting the concentration of oxygen in water body (Hakam et al., 2015). This effect on low photosynthetic activity of aquatic life and increase the oxygen demand thus biological attack process to aquatic plants (Wong, Szeto, Cheung, & McKay, 2004). Although methylene blue is not significantly hazardous to human being, it can contribute some harmful effects. Acute exposure to methylene blue can cause confusion, shortness of breath, vomiting, and headache (Tsai et al., 2009).

2.3 Dye Removal Treatment

Nowadays, various remediation on dye effluents has been carried out in countless studies as the dyes especially MB contained in the wastewater creates negative impacts on human health and ecosystem. Numerous biological degradation, physical separation and chemical treatment on MB removal was presented in Table 2.1.

Biological treatment is using incorporation of aerobic and anaerobic process to treat dye wastewater (Robinson et al., 2001). Biodegradation treatments including microbial culture (Alhassani, Rauf, & Ashraf, 2007), enzyme degradation (Bilal, Asgher, Iqbal, Hu, & Zhang, 2017), algae degradation (Kousha, Daneshvar, Esmaeli, Jokar, & Khataee, 2012), fungal (Lade, Waghmode, Kadam, & Govindwar, 2012) as well as mixed microbial culture (Kumar et al., 2006) are widely used in treatment. Utilization of biological treatment mainly due to the low price of biological dye removal and can be accomplished easily (Singh, & Arora, 2011). However, it inability to obtain satisfactory colour elimination due to the low biodegradation property of dyes and the instability of biological treatment as reaction changeable at times (Katheresan, Kansedo, & Lau, 2018).

Chemical methods are applied using its theories in removing dye components. The common chemical methods of dye effluents are coagulation -flocculation (Yue et al., 2008), oxidation (Mishara et al., 2011), and chemical precipitation (Bouyakoub et al., 2011). Chemical methods involve the addition of chemical agents such as ferric sulphate (Merzouk, Gourich, Madani, Vial, & Sekki, 2011), calcium chloride (Khouni, Marrot, Moulin, & Ben Amar, 2011), aluminium sulphate (Khayet, Zahrim, & Hilal, 2011) in process. Chemical methods are efficiency in dyes removal but the expensive cost of

chemicals and generates secondary pollution draws back the application of this technology at industrial scale.

Physical treatment is a straightforward conventional method that carried through the mass transfer mechanism. It also a most common treatment in dye removal due to its efficiency and simplicity of design. Conventional treatment including adsorption (Hameed, Ahmad, & Latiff, 2007; Rafatullah et al., 2010), ion exchange (Tekbaş, Yatmaz, & Bektaş, 2008), irradiation (Lachheb et al., 2002), and reverse osmosis (Nataraj, Hosamani, & Aminabhavi, 2009). Among all these physical treatments, adsorption process is known as most effective method due to its cost-effectives and simplicity in operation and process control effluents.

Table 2.1: MB removal by biological, chemical, and physical treatment with the efficiency removal.

References	Method	Conditions and results	Maximum efficiency(%)
		Biological	
Manju, & Bishnoi (2016)	Adsorption by immobilized rice straw (Microbial biomass)	Maximum dye removal at 1 % adsorbent dosage, dye concentration of 300 mg/L, pH value 7 and at temperature 30 ℃ in 2 days.	88
Al-Ansari et al. (2011)	Algae Degradation (Immobilized *Desmodesmus sp*.)	Maximum dye removal after 6 days contact time when dye concentration was set at 20 mg/L.	98.6
		Chemical	
Hossein, & Rezaee (2015)	Advanced oxidation process with hydrogen peroxide and UV.	The experiment was conducted under shaking conditions. Dye removal was tested with hydrogen peroxide of 1 Mmol, initial concentration of MB of 3, 5 and 10 mg/L, reaction time of 3.5, 4.5 and 10.5 minutes and UV irradiation intensity of 2400 $\mu W/cm^2$. Rate of dye removal became higher as hydrogen peroxide concentration and UV light intensity became higher.	98
Jan, & Hasal (2013)	Photochemical degradation with a combined system of titanium dioxide and UV.	Titanium dioxide was immobilized with polyvinyl alcohol to further enhance dye removal. Ideal process parameters were found to be when initial dye concentration is 20 mg/L, light intensity of UV light at 4 W, liquid volumetric flow rate is 2 mL/min and	99

		wavelength of 254 nm. Reaction time for maximum dye removal was less than 20 hours	
		Physical	
Suteu, Bilba, & Coseri, (2013)	Purolite C145 Macroporous Polymeric Ion Exchange	The mode is experiment is batch adsorption. Tried and tested successful experiment parameters are when contact time is more than 5 hours, initial dye concentration is 29.6 mg/L, initial solution pH is 12, resin dose is 40 g/L and temperature is 20 ℃. The monolayer adsorption capacity of the cation was found to be 31.9846 mg/g.	85
Kavitha, & Namasivayam (2017)	Adsorption on coir pith	The adsorption capacity was found to be 5.87 mg/g by Langmuir isotherm for the particle size 250–500 μm. The equilibrium time was found to be 30 and 60 min for 10 and 20 mg/L and 100 min for 30, 40 mg/L dye concentrations, respectively.	99

2.3.1 Adsorption

Adsorption referred to a phase transfer process that commonly used in removal of the non-degradable organic and inorganic substances from effluent. Adsorption took place when the absorbable solutes (adsorbate) contacted to a solid (adsorbent) with highly porous surface structure where liquid–solid intermolecular forces of attraction occurred (Worch, 2012).

Most characteristic of adsorbent surfaces are energy-rich and active sites. Those characteristics allow interaction with solutes in the adjacent aqueous phase by their specific electronic and spatial properties (Worch, 2012). Basically, active sites have different energies where the surface is energetically heterogeneous. The adsorption theory is presented in Figure 2.2. Adsorbate is referred as the species that will be adsorbed while adsorbent is the solid material that serves the surface for adsorption (Worch, 2012).

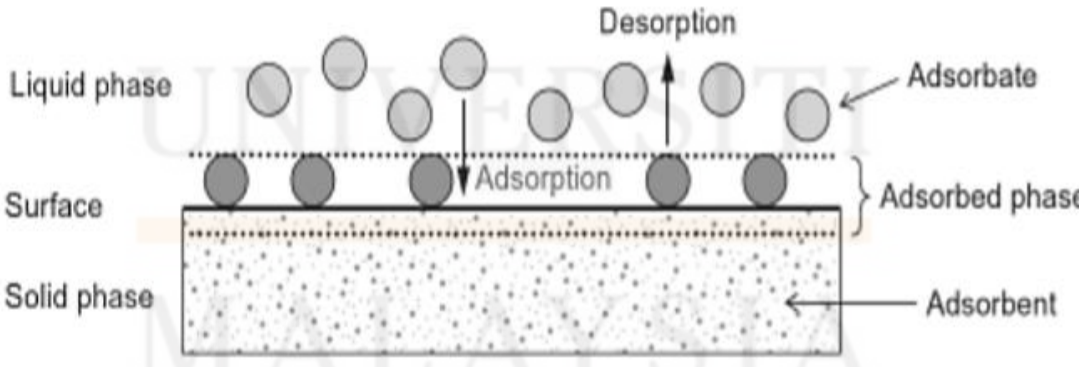

Figure 2.2: Basic process of adsorption.

Source: Worch (2012).

The effectiveness of adsorption was varied by few factors such as the effect of flow rate, contact time, initial concentration adsorbates inlet, adsorbent's dosage and pH value. The term of this reverse process is desorption (Worch, 2012).

2.4 Adsorbents

Adsorbent can be defined as the changes between molecules in a mixture through analysis of kinetics and adsorption equilibrium (Sharifah, 2006). There were two types of adsorbents commonly used, either natural origin adsorbent or the adsorbent that resulted from industrial production and/or activation process. Typical natural adsorbents consisted the clay minerals, natural zeolites, oxides, or biopolymers while engineered adsorbents were classified into carbonaceous adsorbents, polymeric adsorbents and oxidic adsorbents. According to Worch (2012), engineered adsorbents were the adsorbent that exhibited the highest adsorption capacities. They were produced under strict quality control and shown nearly constant properties.

Based on Sharifah (2006), adsorption process by adsorbent can be explain into 3 steps. During step 1, compound diffuse into fluid film and attach on the adsorbent surface. Then, the attached compound (absorbate) migrate from external surface area into the pores of adsorbent through diffusion. This step also known as mixed diffusion due to exist 2 process which are pore diffusion and surface diffusion carry out at the same time. The continuous adsorption process in the pore site occur in step 3. The mechanism of adsorption by adsorbent is illustrated in picture 2.3.

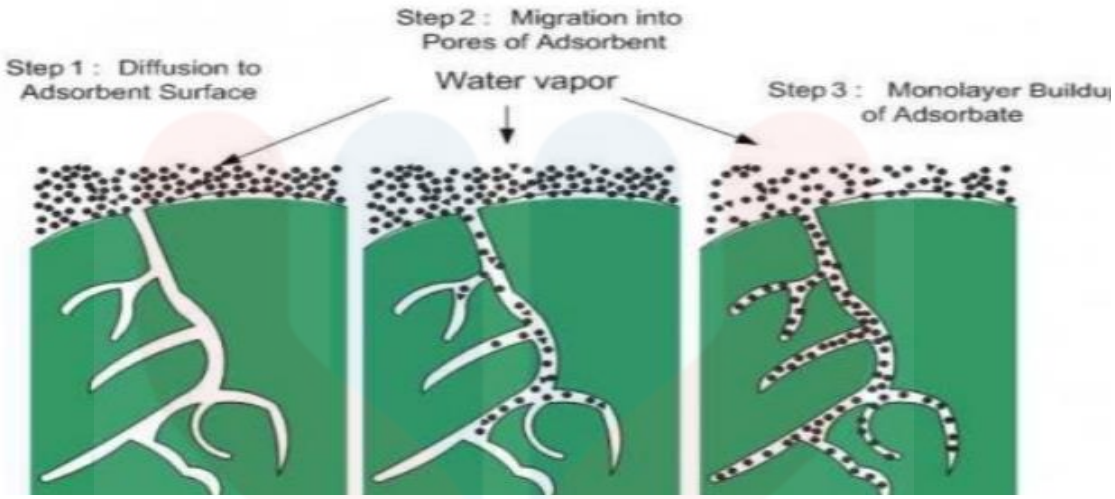

Figure 2.3: Mechanism of adsorption by adsorbent.

Source: Sharifah (2006).

The common adsorbents reported in the literatures using activated carbons because it has high abilities adsorption for a large number of organic and inorganic metal ions (Sanmuga priya, 2017; Wang et al., 2005). However, there are a number of drawbacks in activated carbon such as costly raw material (coal or coke), operational losses due to combustion at high temperature, and hygroscopicity limits treatment in wide range of effluents (Sanmuga priya et al., 2017; Dawood, 2012). Therefore, adsorbents that derived from cost-effective and locally available precursor are needed to substitute activated carbon. Agricultural and industrial wastes are available in large quantities or certain by-products from biomass may have the potential as cheaper adsorbents (Šćiban, Klašnja, & Škrbić, 2008). There are several review articles have been reported in Table 2.2 regarding the use of different biomass adsorbents on MB removal.

Table 2.2: A review of Methylene Blue adsorption capacity of adsorbents derived from biomass.

Reference	Source of Biomass	Adsorption Capacity, Q_m (mg/g)
Mudyawabikwa, Mungondori, Tichagwa, & Katwire (2017)	AC- Tobacco Stalks ($ZnCl_2$/microwave)	1264.51
Laksaci, Khelifi, Trari, & Addoun (2017)	AC- Coffee Grounds (400 ℃,N_2/ KOH/ 800 ℃, N_2)	1058 µmol/g
Cazetta et al. (2011)	AC- Coconut shell (NaOH, 700 ℃, N_2)	916.26
Garcia, Sedran, Zaini, & Zakaria (2017)	AC- Palm Kernel Shell ($ZnCl_2$/ 500 ℃, N_2)	225.3
Yang, Zhu, Zhang, & Xu, (2008)	Rice Husk (Fe_3O_4 coated)	321
Zhou et al. (2014)	Pine Wood Sawdust (H_3PO_4, 80 ℃/ KOH/ 1000 ℃, N_2)	303.03
Ghasemian Lemraski, Sharafinia, & Alimohammadi (2017)	Persian Mesquite Grain (H_3PO_4/ 600 ℃, N_2)	384
Teow, Nordin, & Mohammad (2018)	Graphene- Palm Oil Mill Effluent (H_2SO_4/ 400 ℃)	216.22
Altintig, Altundag, Tuzen, & Sari (2017).	AC and magnetic AC (Fe-AC) from acorn shell ($ZnCl_2$/ 700 ℃/ addition of Fe_3O_4)	303(AC) 357.1 (Fe-AC)

2.5 Biocarbon

Biocarbon, a solid carbonaceous carbonized from plant-biomass or biomass has received overwhelming attention in environmental remediation due to its efficient adsorption, binding affinities of organic and inorganic contaminants, and environmental-friendly approach property (Ahmad et al., 2012). Lehmann and Johnson (2009) defined biocarbon as "carbon-rich, fine-grained, porous substance, which is produced by thermal decomposition of biomass under oxygen-limited conditions and at relatively low temperatures (<700 ℃)". The well-developed pore structures of biocarbon make it more suitable used in water treatment (Verheijen, Jeffery, Bastos, Van der Velde, & Diafas, 2010).

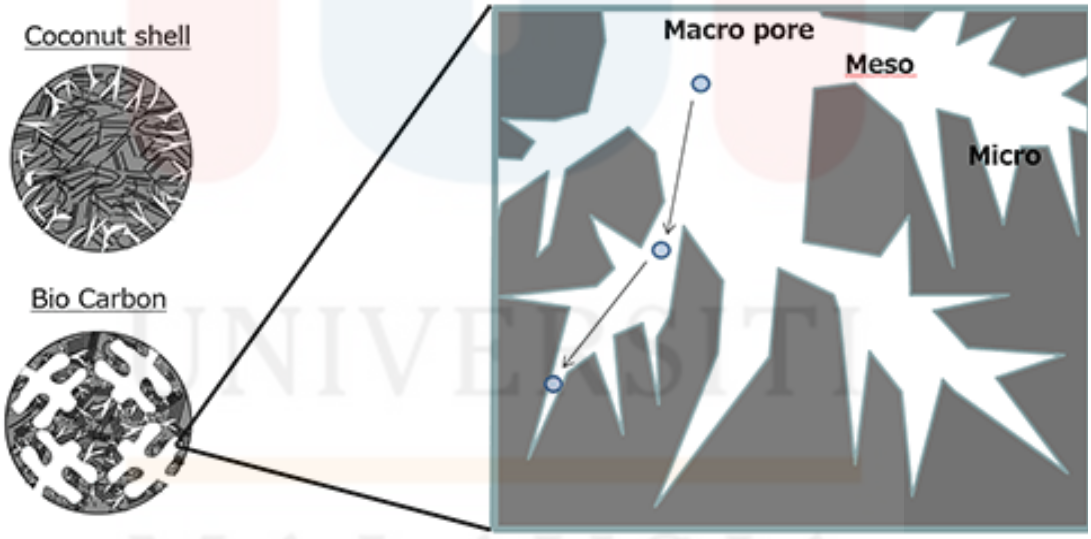

Figure 2.4: Pore structure illustration of biocarbon.

Source: Maneerung et al. (2016).

The biomass feedstocks used as well as the production technique may substantially affect biocarbon's physical and chemical properties (Brewer et al., 2008).

Several studies showed that precursor selection may affect the biocarbon quality such as feedstock that rich in oxygen but lack of hydrogen develop a close cross-linkage and resulting compact mass. However, temperature of heat treatment will be the mostly influence in quality biocarbon compared to the precursor (Luglio, 2018).

Biocarbon with high specific surface area and structure received a bulk of studies focused on its application such as soil amendment to improve soil fertility, mitigate climate change by sequestering carbon dioxide, energy production including syngas and bio-oil, and adsorbent for dye and heavy metal removal from wastewater (Luglio, 2018). Biocarbon from bamboo (Yang, Lin, Wei, Zhao, Wang, 2013), crop residues (Xu, Xiao, Yuan, & Zhao, 2011), digestion residue, palm bark, and eucalyptus (Sun, Wan, & Luo, 2013) have been emerged as adsorbent for adsorption of dye compounds. Yang et al. (2013) reported that the biocarbon prepared from bamboo performed an excellent adsorption of metal complex dye, acid black 172 from aqueous solution even at high ionic strength. Crop residues from canola straw (CS), soybean straw (SS), peanut straw (PS), and rice hulls (RH) were slowly paralyzed for 4 h at 530 ℃ to generate their respective biocarbon (Xu et al., 2011). The removing methyl violet have been reported by the capacities of adsorption followed the orders CS> PS> SS> RH which was parallel to their respective cation exchange capacities. While Sun et al. (2013) produced biocarbon prepared from palm bark (BC-PB), eucalyptus (BC-E) and anaerobic digestion residue (BC-R) for used as sorbents for removal of cationic methylene blue dye (MB). The efficiencies of MB removal in the samples with initial concentrations of 5 mg/L at pH 7.0 by BC-PB, BC-R, and BC-E after 2 h were 99.3%, 99.5%, and 86.1%, respectively.

Various studies show that biocarbon and its activated derivatives improve adsorption capability of different contaminants. Aside from activation, magnetization also another effective technique to improve biocarbon property which discussed later.

The high efficiency to remove multiple contaminants in aqueous solution makes biocarbon an ideal adsorbent or precursor material for water treatment. Lastly, biocarbon technology which more agronomic co-benefits and multiple environmental compared with the existing low-cost water treatment methods encourage more and more investment on biocarbon (Hale et al., 2012).

2.6 Activated Biocarbon (AC)

Agricultural waste materials are economic and eco-friendly due to their large quantities, cheap, unique chemical composition, and renewable nature are sustainable option for wastewater treatment. The low ash content and reasonable hardness of waste produced added value for AC production (Ahmedna et al., 2000). AC is produce through raw material dehydration and carbonization followed by chemical, physical or physicochemical activation.

AC has been proven to be an effective adsorbent use in wastewater treatment due to the effectiveness in eliminating various organic and inorganic species from environmental pollutants (Namasivayam & Kavitha, 2002). It was reported that AC contained internal surface areas > 500 m^2/g compared to 10 m^2/g for the precursor biocarbon (Mohan, Sarswat, Ok, & Pittman, 2014). The well-developed structures of AC such as large surface area, high porosity, variable characteristics of functional groups present on the surface, and high degree of pore structure make it a useful material that not only employed as adsorbents for environmental pollution control and also as catalyst purification in chemicals (acids, amines, glycerine), clothing, cosmetic, and petrochemical industries (Cecan et al., 2012).

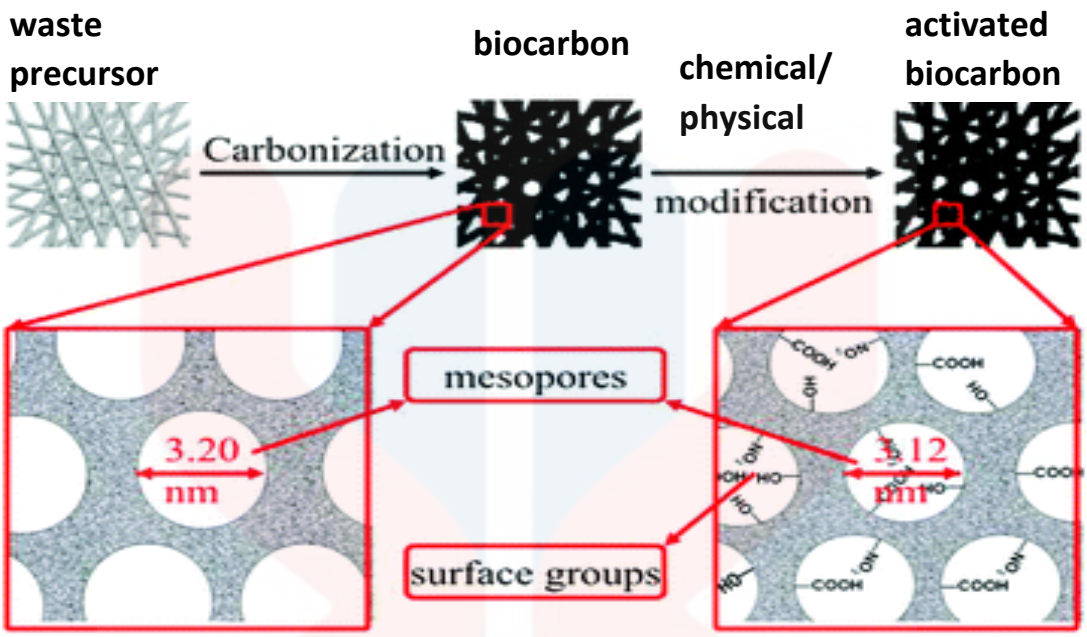

Figure 2.5: The preparation procedure and the mesoporous structure of AC.

Source: Liu et al. (2012).

A wide range of waste materials obtained from agricultural by products have been explored as AC including coconut shell (Gratuito, Panyathanmaporn, Chumnanklang, Sirinuntawittaya, & Dutta, 2008), almond (Christopher, & Wayne, 2002), rice husk (Khalid, Ahmad, Toheed, & Ahmed, 2000), bamboo (Hameed, Din, & Ahmadand, 2007), sugar beet bagasse (Önal, Akmil-Başar, Sarıcı-Özdemir, & Erdoğan, 2007), and orange peel (Li et al., 2008). For example, the adsorption of 2,4,6-trichlorophenol (TCP) on coconut husk based AC synthesized under optimized conditions was assessed by Tan, Ahmad, & Hameed (2008). Adsorption capacity of TCP was found to increase with increase in agitation time and initial concentration. The maximum monolayer adsorption capacity of 716.10 mg/g was observed at 30 ℃. The adsorption mechanism was determined from the intraparticle diffusion model. Boyd plot revealed that the adsorption of TCP on the activated carbon was mainly governed by particle diffusion. Regmi et al.

(2012) also synthesized activated biocarbon from switch grass via hydrothermal carbonization (HTC) and alkali activated HTC biocarbon (HTCB) for evaluating the adsorption of copper and cadmium from aqueous solution. Results showed that the HTCB performed up to 100 % copper and cadmium removal which higher than result obtained from HTC biocarbon (16 % for copper and 5.6 % for cadmium). Therefore, they concluded that activation process may improve the sorption properties and porous structure.

2.7 Magnetic Activated Biocarbon (MAC)

In recent years, the application of magnetic particle technology to resolve environmental pollutions have received extensive attention. Ferromagnetic nanoparticles of iron oxides including maghemite (γ-Fe_2O_3) and magnetite (Fe_3O_4) have been widely employed as magnetic material due to their excellent magnetic properties, biocompatibility, and chemical stability compared with metallic magnetic materials. (Chen, Hu, Shao, Li, & Wang, 2009). They are efficiently to adsorb large amounts of contaminants from aqueous or gaseous effluents in short time period without producing any by-products or secondary pollution (Rodr ǵuez-Couto, Osma, & Toca-Herrera, 2009). Magnetic particles can be separated from the medium by external magnetic field after the adsorption process.

Maghemite, γ-Fe_2O_3 particles have been widely used as effective sorption agent for numerous chemical compounds including organic dyes, heavy metals, and antibiotics (Xu, Xiao, Yuan, & Zhao, 2011; Zhu et al., 2011). However, Wong, Ngadi, Unuwa, & Hassan (2018) reported that "γ-Fe_2O_3 particles contained high surface energy arising from strong van der Waals forces, therefore it has a tendency to form aggregates in aqueous

solutions which dramatically decrease the surface area and adsorption abilities as well as increase the cost". Biocarbon which generated by pyrolysis of carbon rich biomass is potential support to further enhance the stability of γ-Fe_2O_3 particles due to it widely available, cheap, and high porosity structure. In addition, the rich oxygen-containing functional groups and high ion exchange capacity on biocarbon surface is ideal for reducing metal bioavailability and leachability (Luo & Zhang, 2009).

Xu, & Chen (2013) developed three magnetic biocarbon (MOP250, MOP400, MOP700) by chemical co-precipitation of Fe^{3+}/Fe^{2+} on orange peel powder and subsequent under different temperatures (250 ℃, 400 ℃, and 700 ℃) for pyrolysis. Prepared samples were applied to aqueous phosphate, naphthalene and p-nitrotoluene remediation. MOP400 performed the best sorption capability for organic pollutants compared with non-magnetic biocarbon (OP400). The same was true for phosphate adsorption, with magnetic biocarbon, especially MOP250, showing much higher sorption capability as compared to the companion non-magnetic biocarbon. As a result, magnetization is indicated as alternative way improved sorption ability of biocarbon.

A novel magnetic cellulose/ Fe_3O_4/ activated carbon (m-cell/ Fe_3O_4/ ACCs) was prepared by co-precipitation of ferric and ferrous salts was used to study the adsorption Congo-red from aqueous solution (Zhu et al., 2011). The maximum Congo-red adsorption capacity of m-cell/ Fe_3O_4/ ACCs was compared with others low-cost adsorbents including N,0-CMC-MMT prepared by Wang, & Wang (2008) and waste red mud adsorbent by Namasiwayam, & Nasrazarasi (2008). It showed m-Cell/ Fe_3O_4/ ACCs contained a good adsorption capacity (66.091 mg/g) compared to others adsorbents which contained 64.24 mg/g and 4.05 mg/g respectively.

2.8 Cethyltrimethylammonium Bromide (CTAB)

A cationic surfactant, CTAB (IUPAC name: hexadecyl-trimethyl-ammonium bromide) has molecular formula $C_{19}H_{42}BrN$ with molar mass 364.45 g/mol. It contained a long hydrocarbon chain and is one of the most popular cationic surfactants that found in many household products such as shampoo and cosmetics. The application of CTAB was also found in biological field for medical (Illert, Wangler, Wangler, & Roder, 2017), protein electrophoresis (Rabilloud, 2016), and DNA extraction (Mirimin, & Roodt-Wilding, 2015) used due to the cetrimonium cation is an effective antiseptic agent against fungi and bacteria (Nouqabi, Zargar, Takassi, & Moradi, 2017).

Figure 2.6: Chemical structure of CTAB.

Source: Maki, Sagara, & Kawai (1991).

There are a few papers were found application of CTAB for wastewater treatment. For example, Zargar Parham, & Hatamie, (2009) reported that iron oxide nanoparticles coated with cetyltrimethylammonium bromide (CTAB) performed as a high efficient adsorbent for removal of amaranth (AM) from water. Mohamed (2004) prepared an adsorbent, CTAB-modified mesoporous molecular sieve FSM-16 for acid dye (acid blue, and acid yellow) removal and compared it efficiency with non-treated FSM-16 and activated carbon (AC) derived from rice husk. As result, CTAB modified FSM-16

presented a better adsorption than former FSM-16 and AC at low concentration of acid dyes. The high performance of CTAB/ FSM-16 at low concentration is indicated CTAB could narrow the pore opening but maintenance of a significant portion of the pore volume. This also been confirmed through TG test that CTAB/ FSM-16 performed a higher hydrophobicity than CTAB-free FSM-16 samples.

2.9 Cyclopentasiloxane (CPS)

CPS is a cyclic (circular) volatile methyle siloxane, which commonly known as Decamethylcyclopentasiloxane (D5). It is classified as a cyclomethicone with empirical formula $C_{10}H_{30}O_5Si_5$ and molecular weight 370.8 g/mol. The IUPAC name is given as Decamethyl-1,3,5,7,9,2,4,6,8,10-pentaoxapentasilecane. CPS It has a wide application use across multitude personal care products such as antiperspirants, sun protection products, personal lubricants, skin, hair and nail care formulations, and fragrance and cosmetic preparations (Montemayor, Price, & Van Egmond, 2013).

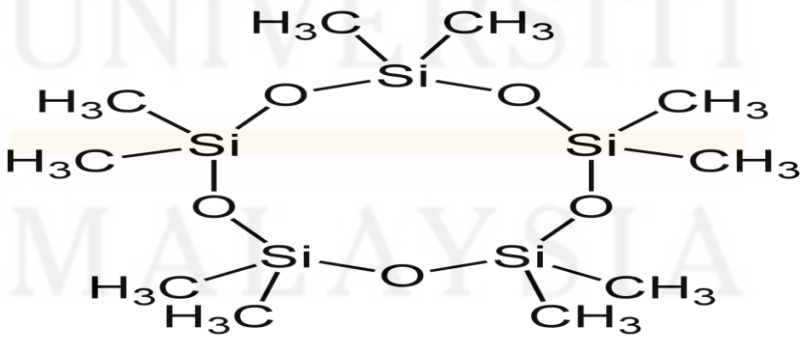

Figure 2.7: Chemical structure of CPS.

Source: Johnson et al. (2011).

There is one study found conducted by Starch, Fiori, & Lin (2003) that properties of CPS might contributed to the extended structure of elastomers and capability adsorb large amount of silicone fluid. They further explained that "when the elastomer is synthesized in CPS, the elastomer and CPS form what is essentially one large gel in the reaction vessel. This gel is then sheared to produce gel particles that thicken silicone oils in much the same way that carbomer gel particles thicken aqueous formulations. These soft gel particles are what provide the unique aesthetic properties in many formulations". In addition, one of the biggest benefits that CPS provided is the economical for manufactures of products. It potential to become cost-effective substitute compare to others. Increasing efforts have been devoted to the potential applications of CPS as its concentration can be more easily varied due to it is a synthetically manufactured. The low viscosity property makes it more suitable to apply in wastewater treatment as it wouldn't leave secondary pollution which may cause negative impact to environment.

CHAPTER 3

METHODOLOGY

3.1 Materials

Chemical and Reagent

Activated Biocarbon (with particle size <45 mesh), Cetyltrimethylammonium bromide (CTAB), Cyclopentasiloxane (CPS), Distilled Water, Iron (III) Oxide Powder, Iodine pearl, Methylene Blue, Potassium Iodide, Sodium Carbonate, Sodium Hydroxide, Sodium Thiosulfate, Starch.

Apparatus and Equipment

Amber bottle, Aluminium Foil, Beaker, Burette, Burette Stand, Bruker D2 Phaser, Daihan WUC-D22H Digital Ultrasonic Cleaner, Dropper, Electric weight, Erlenmeyer flak with stopper, Fume hood, Glass rod, Glove, Hot Plate, JEOL Model JSM IT-100

equipped with an Energy-Dispersive Spectroscopy (EDS), Mask, Magnet, Measuring Cylinder, Memmert Oven UF110, Mettler Toledo TGA/DSC 2 (SF), Micropipette (100-1000 µL), Moisture Analyser, Orbital Shaker, pH meter, Pipette Tips, Thermo Scientific GENESYS 20, Thermo Scientific Nicolet iN10 Infrared Microscope & iZ10 FTIR module, Reagent Bottle, Sieve Shaker, Spatula, Sieve Pan, Test tube with Lid, Volumetric Flask, Zip log bag.

3.2 Methodology

Iron (III) oxide powder and AC which provided by supervisor were used to synthesize magnetic activated carbons by a simple process. The iron oxide combined with AC was designed as MAC while cross-linked CTAB and CPS embedded MAC were designed as MAC-CTAB and MAC-CPS respectively. The AC and magnetic activated carbon provided (pMAC) by supervisor were selected as positive and negative control respectively in this study. The methodology flow chart of this study was illustrated in Figure 3.1.

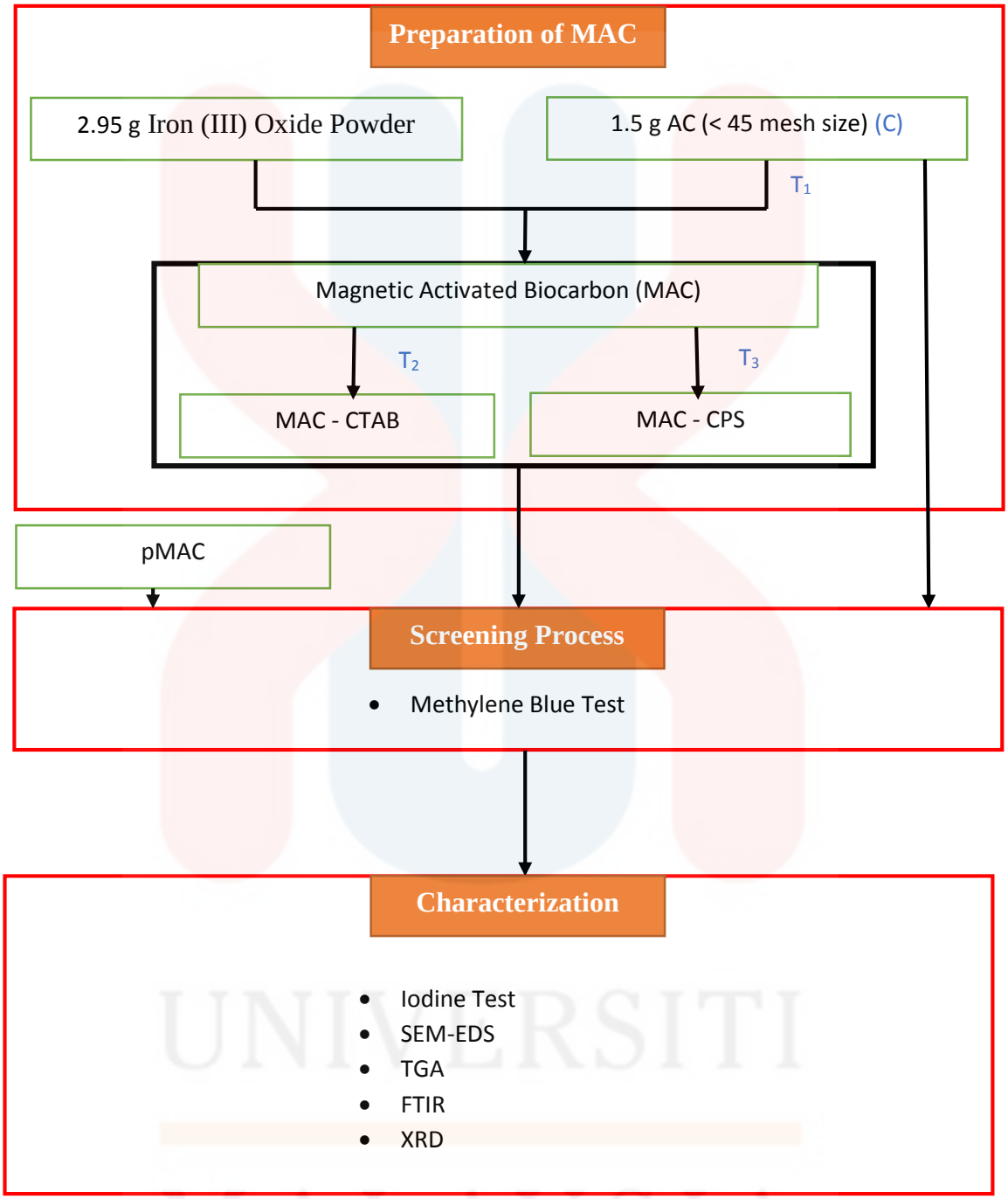

Figure 3.1: Schematic of the MAC Study.

LEGEND:

C : Control

T_1 : Treatment 1

T_2 : Treatment 2

T_3 : Treatment 3

3.2.1 Development of MAC

In this procedure, 45 mL of distilled water was added into 250 mL flask containing 2.95 g of magnetite powder and followed by agitating at 250 rpm at 30 ℃. After 30 min of mechanical shaking, 1.5 g of AC was added into the magnetic fluid and continuously shake for 5 min. Afterward, 0.6 mL of cross linker was introduced into mixture and shaking for 60 min. The mixture was transferred to sonicated bath (amplitude: 80%) for another 60 min to achieve a uniform mixed solution. After completion of reaction, MAC was cooled to room temperature and washed with distilled water until a pH range between 6 to 7. MAC was isolated from mixture by using magnet and dried at 50 ℃ in an oven, stand by to application.

The MAC yield was defined as the final weight of product after magnetization, washing, and drying. The percent yield was determined by the Formulae 1:

$$Yield\ (\%) = \frac{Wc}{Wo} \times 100 \qquad (1)$$

where W_c stand for final MAC (T_1/ T_2/ T_3) dry weight (g) while W_o is the AC dry weight (g), respectively (Cazetta et al., 2011).

3.3 Methylene Blue Test

3.3.1 Preparation of Methylene Blue (MB) Solution

A stock solution of MB (1000 ppm) was prepared by dissolving 1.219 g of dye in 1000 mL of double distilled water (Meghavathu, Kumari, & Vangalapati, 2017). Aqueous solutions with 5 ppm was prepared by successive dilution of the stock solution with water. All the solutions were prepared using double distilled water. The initial concentration (C_i) of MB was obtained by measuring O.D at 666 nm (Deng, Yang, Tao, & Dai, 2009) with a spectrophotometer (Thermo Scientific GENESYS 20). The calibration curve was obtained from the spectra of the standard solutions (0–10 ppm).

3.3.2 Visual Demonstration Adsorption Experiment

A visual demonstration of MB removal onto prepared adsorbents (MAC, MAC-CTAB, and MAC-CPS) were performed by mixing 0.100 g samples with 50 mL methylene blue aqueous solution (5 mg/L). The mixture was shaken in the rotary orbital shaker for 1 h at room temperature to investigate whether the adsorbents could effectively remove the colour of the solution.

3.3.3 Methylene Blue Adsorption Test

Methylene blue adsorption tests were conducted by mixing 0.100 g of the prepared MAC samples with 50 mL (Zhang et al., 2013) of 5 mg/L methylene blue solution in 250 mL conical flask. Adsorption experiment was carried out at room temperature (24 ± 1 ℃) under shaken at the constant agitation speed (200 rpm) (Kannan & Sundaram, 2001) in a rotary orbital shaker. At different time intervals (range 10 - 60 min), the conical flask was withdrawn and the mixtures were separated from the solution by magnetic separation. Then, 1 mL of solution was sucked by pipette into cuvette and measured as final concentrations (C_f) at 666nm using spectrophotometer (Thermo Scientific GENESYS 20). The dye removal efficiency and adsorption efficiency (Q_e) were calculated by Formulae 2 and 3 respectively:

$$Percentage\ Removal\ (\%) = \frac{100\ (Ci - cf)}{Ci} \quad (2)$$

$$Adsorption\ Efficiency\ (\frac{mg}{g}) = \frac{(Ci - Cf)V}{w} \quad (3)$$

where C_i and C_f are the initial and final concentrations (in mg/L) of dye, V (L) is the volume of solution, and w (g) is the mass of samples used. Blanks containing distilled water was used as control for each batch of experiments. The reading of absorbance was conducted in triplicate and the average values runs were obtained and analysed.

3.4 Characterization of Adsorbents

The physical and chemical properties of adsorbents were studied respectively. Physical properties of studied samples characterized by using Iodine Test, Scanning electron microscopy equipped with energy-dispersive spectroscopy (SEM-EDS), Thermogravimetric analysis (TGA), while chemical properties was analysed through Fourier transform infrared spectroscopy (FTIR), and X-ray diffraction (XRD).

Physical Properties

3.4.1 Iodine Number

3.4.1.1 Preparation of Sodium Thiosulfate

A 0.050 N of sodium thiosulfate was prepared by dissolving 12.410 g of sodium thiosulfate in boiled distilled with approximately 75 ± 25 mL. A 0.10 ± 0.01 g of sodium carbonate was added into the solution to minimize the bacterial decomposition. After cooled to room temperature, the mixture was transferred into a 1 L volumetric flask and diluted by distilled water until the mark. The solution was stored in an amber bottle and left for 4 days to stand before standardizing (ASTM D4607- 94, 2006).

3.4.1.2 Preparation of Standard Iodine Solution

The procedure of preparation is following ASTM D4607- 94 (2006). Around 0.010 N of iodine solution was prepared by mixing 12.700 g of iodine and 19.100 g of potassium iodide (KI) with 2 to 5 mL of distilled water for well mixing mixture. Distilled water was continuously added into the beaker with small increment each time (approximate 5mL) until the total volume of solution reach 50 to 60 mL. The solution was stood with magnetic occasional stirring to allow all crystals completely dissolved for 4 h. Then, the solution was transferred into a 1 L volumetric flask and filled with distilled water until it reached the mark. The solution was stored in an amber bottle before standardizing.

3.4.1.3 Preparation of Starch Solution

A 1.0 $\pm$ 0.5 g of starch was mixed with 5 - 10 mL of cold water. Then, 25 $\pm$ 5 mL of distilled water was added while stirring to the starch paste. The starch paste was poured into 1 L of boiling water and boiled for 4 to 5 min (ASTM D4607- 94, 2006).

3.4.1.4 Iodine Test

The iodine test defined as the amount of iodine adsorbed by 1 g of carbon at the mg level. A higher iodine test shows higher pore volume available of the sample. The

standard procedure for iodine determination test were referred from ASTM D4607- 94 (2006).

In iodine test, the blank reading was examined by taken 10 mL of iodine solution in conical flask and titrated against 0.05 N sodium thiosulphate solution to a pale yellow. Blue colour was performed after 2 drops of starch solution was added into pale yellow iodine solution. Then, the solution was continuously titrated with sodium thiosulphate till it became colourless. The recorded of burette reading was correspond to blank reading (B).

Around 0.2 g of adsorbents (AC, MAC, MAC-CTAB, MAC-CPS and pMAC) were introduced into flask that contained 40 mL of 0.1 N iodine solution and shaken at 200 rpm in a rotary orbital shaker for 50 ±1 min. Next, the solution was filtered through folded filter paper (Whatman No. 2V) into a beaker. A 10 mL of filtrate was collected and titrated against 0.1 N sodium thiosulphate solution until a pale yellow formed. Then, 2 drops of starch indicator solution were added and titration was carried out drop wise until the blue colour disappear. The burette reading correspond to (A). This experiment was carried out in triplicate to obtained the mean value. The iodine number was express in mg/g and calculated by Formulae 4:

$$Conversion\ factor = \frac{mol\ of\ iodine \times normality\ of\ iodine \times 40}{weight\ of\ adsorbent \times blank\ reading}$$

$$C = B - A$$

$$Iodine\ value = C\ \times conversion\ factor \quad (4)$$

3.4.2 Scanning Electron Microscope (SEM-EDS)

The surface morphology of all the studied samples was characterized by JEOL Model JSM IT-100 equipped with an energy-dispersive spectroscopy (EDS) analyser to determine the elemental composition of the samples. The magnifications used for the analysis of samples were in between range of ×1000 up to ×3000.

3.4.3 Thermogravimetric Analysis (TGA)

Thermal stability of magnetic adsorbents under high temperature with control atmosphere was identified by TGA. In this analysis, TGA was carried out by Mettler Toledo TGA/DSC 2 (SF). Samples were placed in alumina crucible and heated at temperatures ranging from 30 to 980 ℃ under nitrogen atmosphere with 10 ℃/min decomposition rate (Zhu et al., 2011).

Chemical Properties

3.4.4 Fourier Transform Infrared Spectroscopy (FTIR)

The functional groups present on the surface of studies samples were analysed by using FTIR spectrometer (Thermo Scientific Nicolet iN10 Infrared Microscope & iZ10 FTIR module). The measurement of FTIR- ATR were recorded in the range of 500- 4000

cm^{-1}, background correction and 128 scans with atmosphere/ at a resolution 4 cm^{-1} using KBr as a reference.

3.4.5 X-Ray Diffraction (XRD)

X-ray diffraction analyser (XRD) is an analysis technique used to identify crystallographic structures in the sample using Bruker D2 Phaser with radiation (λ = 1.54060 Å) over the 2θ range of 10 – 80 °. Small sample size of powder sample was packed into the sample holder for the analysis after vacuum drying. The XRD diffractogram patterns of samples were conducted by using diffractogram EVA for data analysis. X-ray diffraction (XRD).

CHAPTER 4

RESULTS AND DISCUSSION

4.1 Physical Properties of Newly Prepared Samples

The physical properties including the appearance, colour, and magnetometric of newly prepared samples were observed and presented in Figure 4.1.1.

(a) (b) (c)

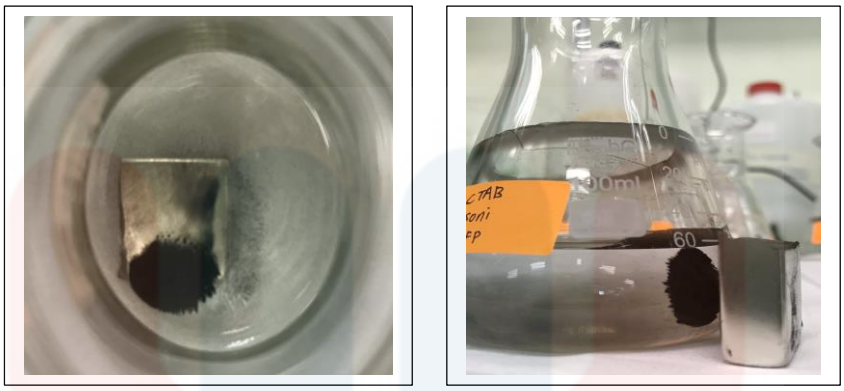

(d) (e)

Figure 4.1.1.: (a), (b), (c) Physical image of MAC, MAC-CTAB, MAC-CPS respectively; (d) The top view of MAC-CTAB; and (e) The side view of MAC-CTAB.

A fine powder with black colour was observed after the synthesized of MAC, MAC-CTAB while MAC-CPS appeared in brownish black. The slightly brown colour performed by MAC-CPS might due to the chemical reaction between CPS and iron oxide. The inconsistence of particle size of MAC-CPS through visual observation due to the incomplete of grinding during preparation process.

Approximate 0.1 g of samples were dispersed in distilled water and a magnet was placed under conical flask to study the magnetic performance. As displayed in Figure 4.1.1, (d) and (e), it showed whole black particles attracted toward magnet, which demonstrated the prepared MAC are high magnetic sensitivity. The excellent magnetic response of prepared MAC to external magnetic field can ascribed to the formed interaction between iron nanoparticle and AC with the help of cross-linker (Korobeinyk, Whitby, Niu, Gogotsi, & Mikhalovsky, 2011). Throughout this simple experiment, it proved that MAC, MAC-CTAB, and MAC-CPS successful magnetize and could be potentially used as a magnetic adsorbent to remove compounds from aqueous solution.

4.2 Production Yield

Production yield is defined as the total mass production of newly prepared MAC produced after complete the preparation process. The amount was calculated and presented in Table 4.2.1. The initial amount used for preparation process was 4.45 g which obtained from 2.95 g of iron oxide powder mixed with 1.5 g of AC.

Table 4.2.1: The Production Yield of Prepared MAC Samples.

Sample	Weight (g)	Yield (%)
MAC (T_1)	6.31	141.57
MAC-CTAB (T_2)	6.24	140.22
MAC-CPS (T_3)	4.95	111.24

The overall production yield of MAC, MAC-CTAB, and MAC-CPS are higher than precursor material which obtained 141.57 %, 140.22 %, and 111.24 % respectively. The yield gained after preparation method can be explained by the addition of iron oxide attached to the porous structure of AC thus increase in the weight as well as yield (Liu et al., 2014). However, the slightly low carbon yield obtained by cross-link treated MACs compare to untreated MAC may because more atoms on the activate site and/or crystal face are consumed for modification. Moreover, the low yield of MAC-CPS among samples could be attributed to the low water solubility property of CPS (Dekant, & Klaunig, 2016). The hydrophobic CPS cross-linked with MAC might be washed away during dilution process.

4.3 Standard MB Calibration

Calibration curve, also known as standard curve is a method for determining the concentration of MB after MAC treatment by comparing to a set of standard MB solution.

Table 4.3.1: Absorbance Readings of Standard MB Solution.

MB Concentration (mg/L)	Absorbance Readings
0	0.000
2	0.352
4	0.704
6	1.042
8	1.328
10	1.603

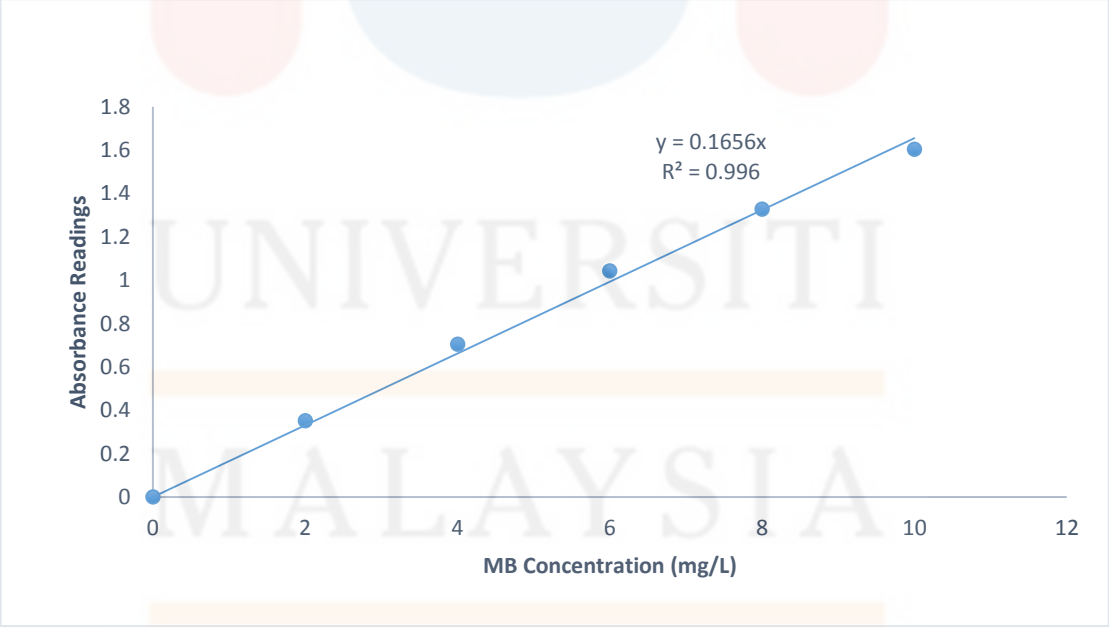

Figure 4.3.1: Standard MB Calibration Curve.

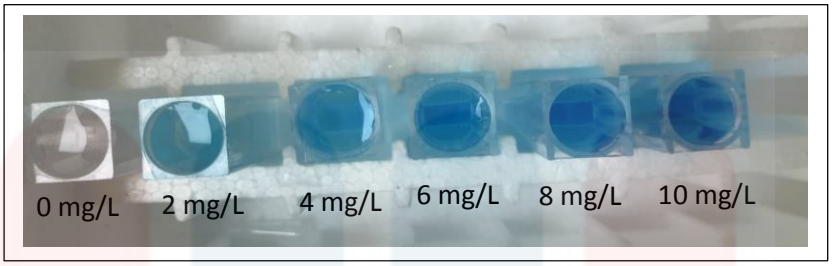

Figure 4.3.2: Standard MB Solution (Ascending order of MB concentration from left).

From Figure 4.3.1, the obtained curve regression equation was y = 0.1656 x with correlation R^2 = 0.996. R^2 value that neared to 1.0 shown the resulting linear regression curve was a positive linear regression curve. The data had tabulated for plotting the MB calibration curve. The absorbance readings which taken from samples can be converted into MB concentration by referring to the curve in Figure 4.3.1. Based on observation in Figure 4.3.2, colour intensity increased along with higher MB concentration. Wavelength of 666 nm was used as it was the region where the blue colour absorbed.

4.4 Adsorption of MB Test

The effect of shaking contact time was carried out using constant concentration of MB solution (5 mg/L) at room temperature. The adsorption of MB ions has been examined onto adsorbents contact time in the range 10 to 60 min.

Table 4.4.1: The effect of contact time MB dye removal efficiency on dye adsorbents.

Treatment	Percentage of Removal (%)					
	10	20	30	40	50	60
	(min)					
AC	91.43	93.24	96.10	95.05	96.14	96.46
MAC (T_1)	95.33	97.79	98.35	98.51	97.83	99.72
MAC-CTAB (T_2)	98.47	97.06	97.83	98.63	99.32	99.24
MAC-CPS (T_3)	95.85	98.87	99.52	99.48	99.36	99.84
pMAC	83.29	90.38	91.30	91.67	91.47	84.06

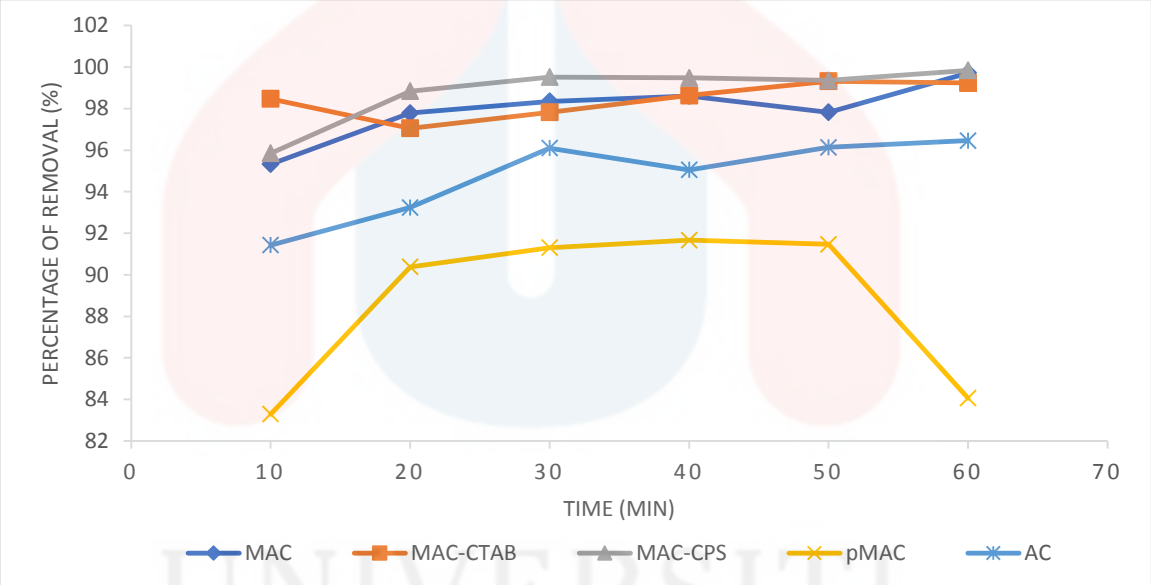

Figure 4.4.1: Time profile of MB adsorption on different adsorbents with MB concentration of 5mg/L at 24 ± 1 ℃.

From Figure 4.4.1. the percentage of removal basically increase with increase contact time. This phenomenon was explained by the adsorption mechanism as MB molecules take time to reach the boundary layer, diffuse into the adsorbent surface, and lastly diffuse into the porous structure. It should be noticed that for magnetic absorbents,

they have two adsorbing sites which are porous structure of carbon (adsorption) and iron oxide nanoparticles (electrostatic repulsion) (Yang et al., 2008).

Among prepared magnetized adsorbents, MAC-CPS showed a better ability, approximate 99.84 % adsorption after 60 min contact time. This can be explained by the CPS contained hydrophobic silica property that help to improve the stability of composite (Kumar et al., 2010) and conventional surface chemistry that functionalized MAC to remove MB ion (Graf, Vossen, Imhof, & van Blaaderen, 2003). The percentage removal of MB by MAC and MAC-CPS showed difference from Table 4.4.1 which contained 99.72 % and 99.84 % respectively. While MAC-CTAB showed slightly lower percentage removal compared to MAC-CPS and MAC as it is a cation surfactant therefore less electrostatic force with MB ions (Gurses, Yalcin, Sozbilir, & Dogar, 2003).

Figure 4.4.1 presented the percentage removal dramatically decreased in pMAC after 50 min mixed of adsorbent and MB solution as the adsorption reached a saturation condition. pMAC which contained magnetic property however showed low efficiency in removing MB ions. This may due to low stability of catalyst used in preparation method thus caused instability of magnetic carbon (Munoz, de Pedro, Casas, & Rodriguez, 2015). Moreover, the inconsistence in percentage removal of samples along the shaking time may due to the different particle size used in test.

Throughout the removal of MB test, the prepared MAC adsorbents performance effectively in removing MB ions from aqueous solution compare to pMAC as well as non-magnetized AC. The efficiency in removing MB follow the orders MAC-CPS > MAC > MAC-CTAB > AC > pMAC. Thus, the prepared MACs are potential to use as sorbents for MB removal treatment.

4.5 Adsorption Capacity

Adsorption capacity of studied samples was calculated with 0.10 g of sample with 50 mL of MB solution. The effect of contact time on the adsorption capacity are depicted in Table 4.5.1.

Table 4.5.1: The influence of contact time on adsorption capacity, Q_e of prepared samples.

Treatment	Adsorption Capacity, Q_e (mg/g)					
	10	20	30	40	50	60
	(min)					
MAC (T_1)	2.38	2.45	2.46	2.46	2.45	2.49
MAC-CTAB (T_2)	2.46	2.43	2.45	2.47	2.48	2.48
MAC-CPS (T_3)	2.40	2.47	2.49	2.49	2.48	2.50
pMAC	2.08	2.26	2.28	2.29	2.29	2.10
AC	2.29	2.33	2.40	2.38	2.40	2.41

Absorption capacity increase with the increase of time. Among the absorbents, MAC-CPS gained the higher which is 2.50 mg/g. MAC which uncross-link treated performed slightly lower adsorption capacity (2.49 mg/g) with MAC-CPS after 60 min of shaking process. Therefore, it was indicated CPS and CTAB cross-linked MAC brings minor influence in adsorption capacity. However, all the prepared MACs enhanced the adsorption capacity to nearly 20 % compared to pMAC. Approximate 5 % of adsorption capacity less by AC compared to prepared MAC adsorbents. Based on literature reports, AC is likely to have a poor adsorption capacity for removal contaminants compare with magnetic adsorbent. It also reported by Pillay, Cukrowska, & Coville (2009) that one of the disadvantages of using AC is that it would limit the adsorption of hydrophilic (MB

ions) substances. Overall adsorption capacity was as follows: MAC-CPS > MAC > MAC-CTAB > AC > pMAC.

4.6 Iodine Test

The pore volume available among absorbents were investigated through iodine number. The residual iodine concentration was examined by titration with standard $Na_2S_2O_3$ solution. The higher the iodine number indicated a higher micro-porosity available.

Table 4.6.1: Effect of cross-linker on iodine number of MAC.

Treatment	Iodine Number (mg/g)
AC	1007.01
MAC (T_1)	240.48
MAC- CTAB (T_2)	255.51
MAC- CPS (T_3)	90.18
pMAC	459.99

It is seen from Table 4.6.1 that MAC which impregnation of iron oxide on precursor material (AC) leading to decrease of iodine number from 1007.01 mg/g to 240.48 mg/g. The decrease was because of iron oxide has a relatively small microporous volume and surface area presented in the composites thus caused a decrease of microporous volume surface area of the composites (Oliveira et al., 2002). As compared to uncross-linked MAC, MAC-CTAB was found to having further increased pore volume. It might due to properties of CTAB cross-linker as being amphipathic in nature surfactant (Nadeem et al., 2006). Whereas the poor porosity of MAC-CPS attributed to the covering

of AC surface by silicon oxide and iron oxide nanoparticles which further evidence by the SEM results. When compare with pMAC, newly prepared MAC showed a low pore volume which might due to the different preparation process.

4.7 Scanning Electron Microscope (SEM)

The surface morphology images of AC, MAC, cross-linked MACs, and pMAC by using characterized by JEOL Model JSM IT-100 was illustrated in Figure 4.7.1.

a)

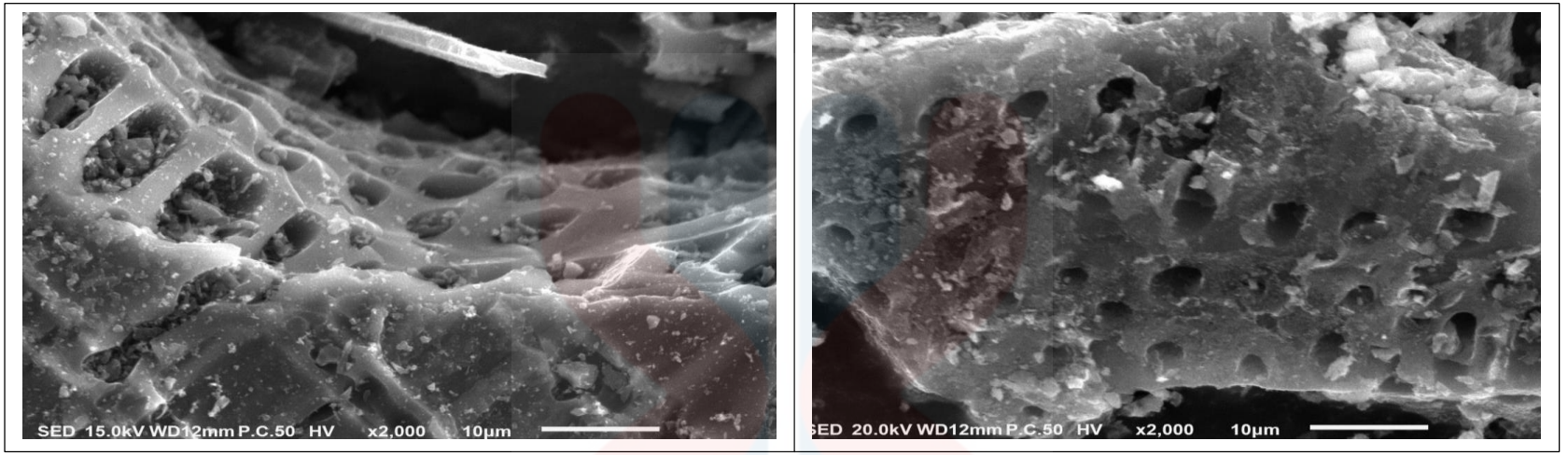

b)

Figure 4.7.1: (a) The SEM characterization of AC, and (b) pMAC under ×2000 magnification.

a)

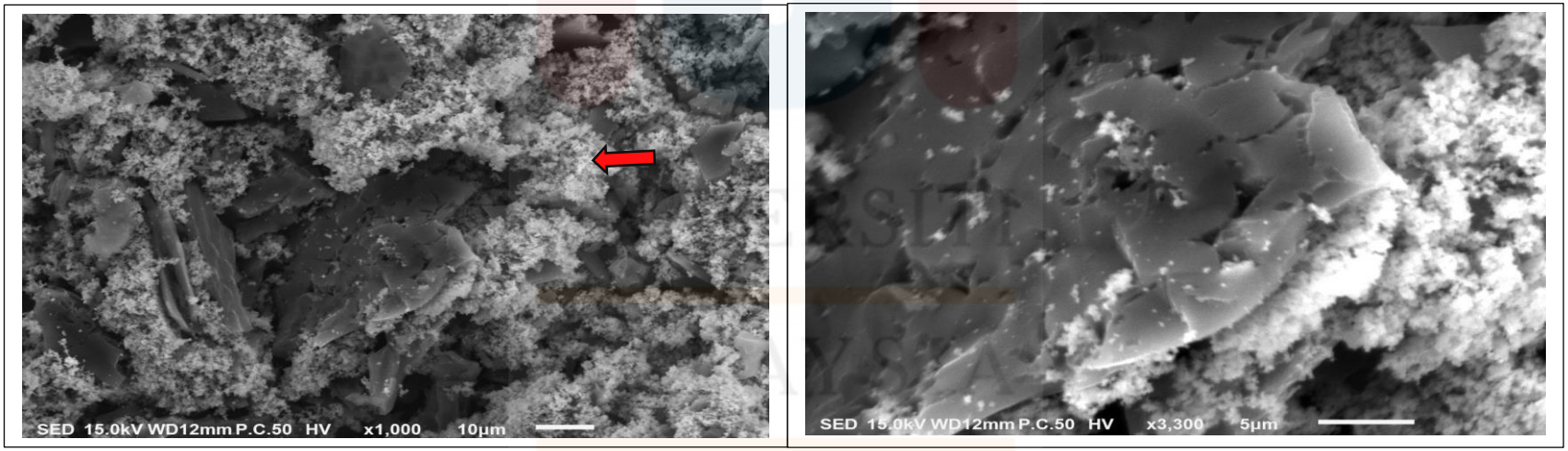

b)

Figure 4.7.2: (a) The SEM characterization of MAC under ×1000, and (b) ×3000 magnification respectively.

a) 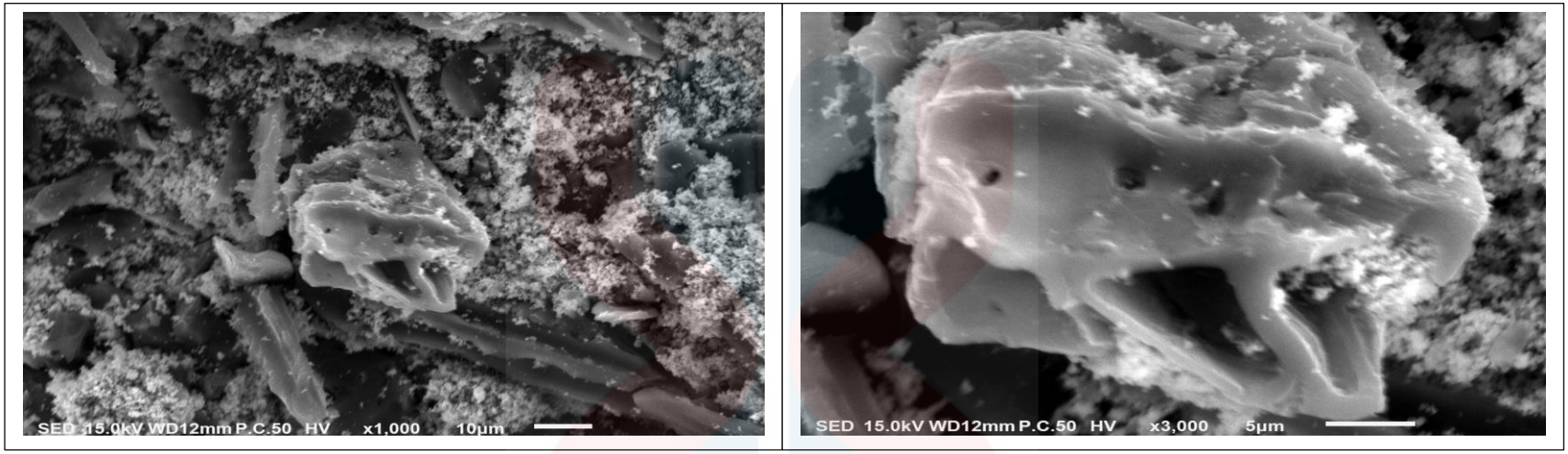

b)

Figure 4.7.3: (a) The SEM characterization of MAC-CTAB under ×1000, and (b) ×3000 magnification respectively.

a) 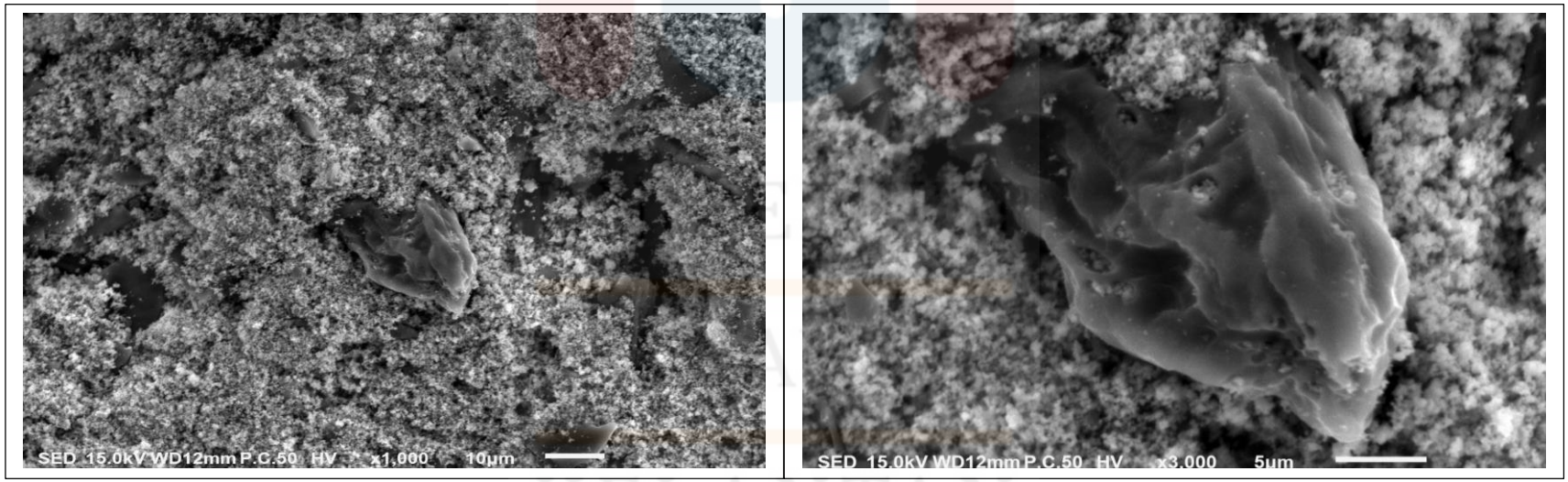

b)

Figure 4.7.4: (a) The SEM characterization of MAC-CPS under ×1000, and (b) ×3000 magnification respectively.

As shown in Figure 4.7.1 (a), abundant of pores observed on the raw AC given further confirmation of the structures of composite with amorphous and porous structure. Some small white particles were spotted on the surface and in the pores AC might attributed to the impurities of provided sample. While Figure 4.7.1 (b) showed pMAC contained large amount of pore volume with a few white particles.

The morphological changed can be observed in Figure 4.7.2 (a) as appeared bright (pointed by arrow) coverage on surface of AC. Further analysis of the micrograph under magnification ×3000 depicted in Figure 4.7.2 (b) showed reduction in porous structure. Thus, it suggested the formation of magnetic nanoparticles impregnation on the AC surface resulted smaller pore volume structure compared to AC. The similar micrograph for AC/Fe oxide composite was reported elsewhere by Zhou et al. (2014). In addition, the micrograph showed that the structure and shape of iron oxide almost similar to each other therefore increase the difficulty in identifying between Fe_3O_4 and γ-Fe_2O_3.

A micrograph of MAC-CTAB with low magnetization (×1000) was illustrated in Figure 4.7.3 (a) portrayed the coverage of magnetic nanoparticle on the surface of MAC however existence of many open loose pores on the surface. A macropores (size above 500-1000 nm) scattered with small amount magnetic nanoparticles micrograph was clearly observed with higher magnification (×3000) in Figure 4.7.3(b).

While the morphology of MAC-CPS under magnification ×1000 showed in Figure 4.7.4 (a) revealed a homogeneous surface distributed by magnetic nanoparticles on AC. Micrograph in Figure 4.7.4 (b) clearly visible that the porous carbon matrix fully filled with agglomerate of magnetic nanoparticles. The morphology obtained explained the low iodine number gained in test.

While compared with newly prepared MACs showed, pMAC showed more pores volume with less amount of white particles indicated less iron oxide contained on pMAC. Therefore, newly prepared MAC samples were suggested a stronger magnetic force than pMAC.

4.8 SEM Equipped Energy-Dispersive Spectroscopy (SEM-EDS)

The EDS spectrum and summary for the elements composition was presented in Figure 4.8.1 for AC, MAC, MAC-CTAB, MAC-CPS, and pMAC.

a)

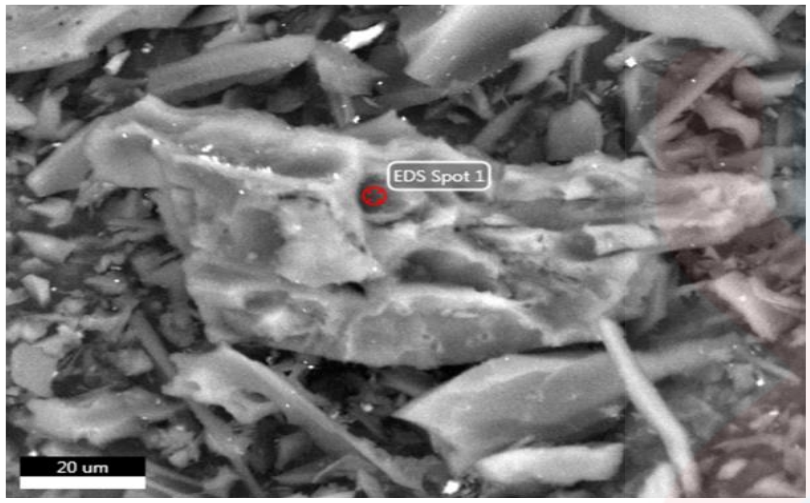

AC		
Element	Weight (%)	Atomic (%)
C K	88.84	91.44
O K	10.99	8.49

Figure 4.8.1: (a) The EDS spectra of AC.

b)

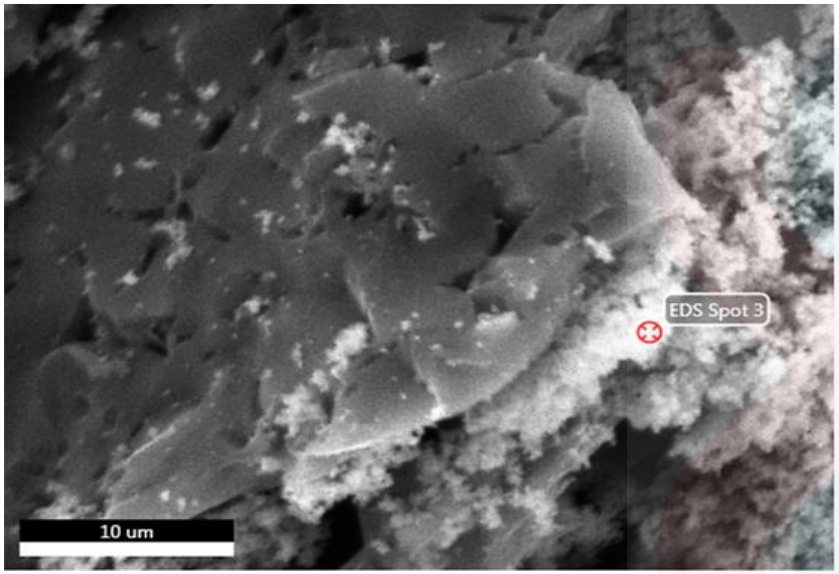

MAC		
Element	Weight (%)	Atomic (%)
C K	12.19	28.63
O K	21.50	37.89
FeK	66.31	33.48

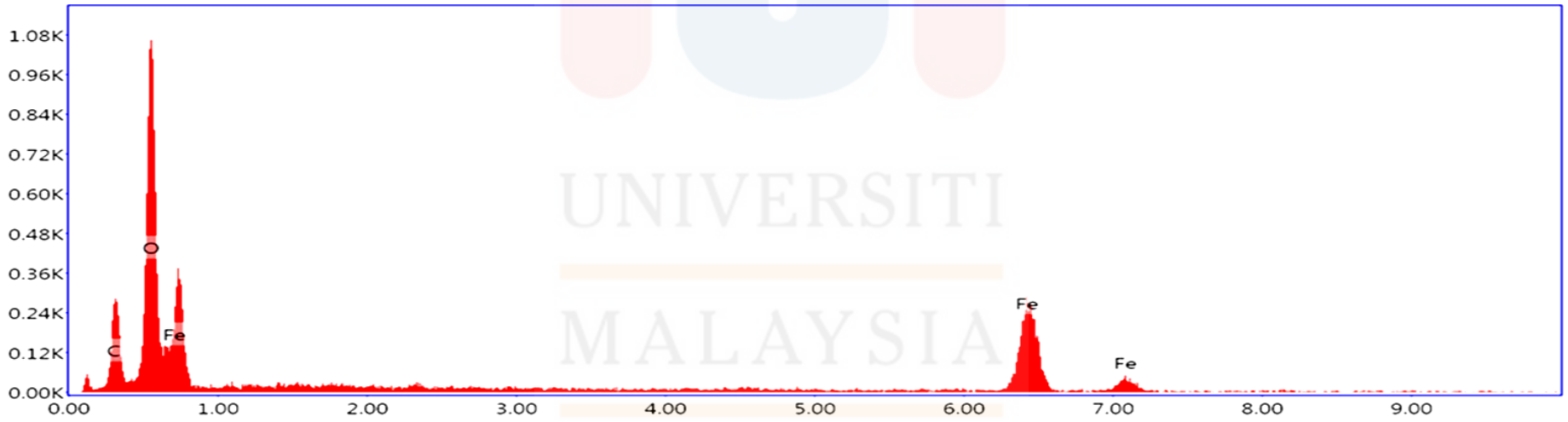

Figure 4.8.1: (b) The EDS spectra of MAC.

c)

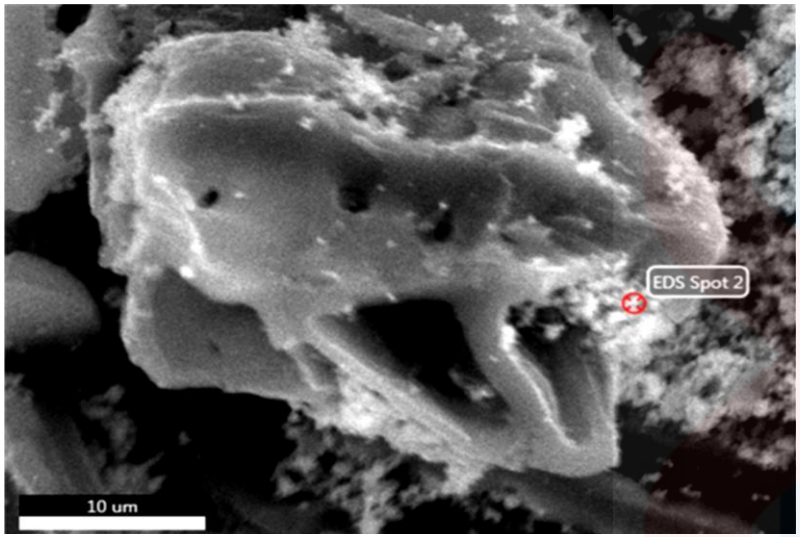

MAC-CTAB		
Element	Weight (%)	Atomic (%)
C K	11.72	25.52
N K	4.35	8.45
O K	19.99	33.96
BrL	0.31	0.11
FeK	63.62	30.96

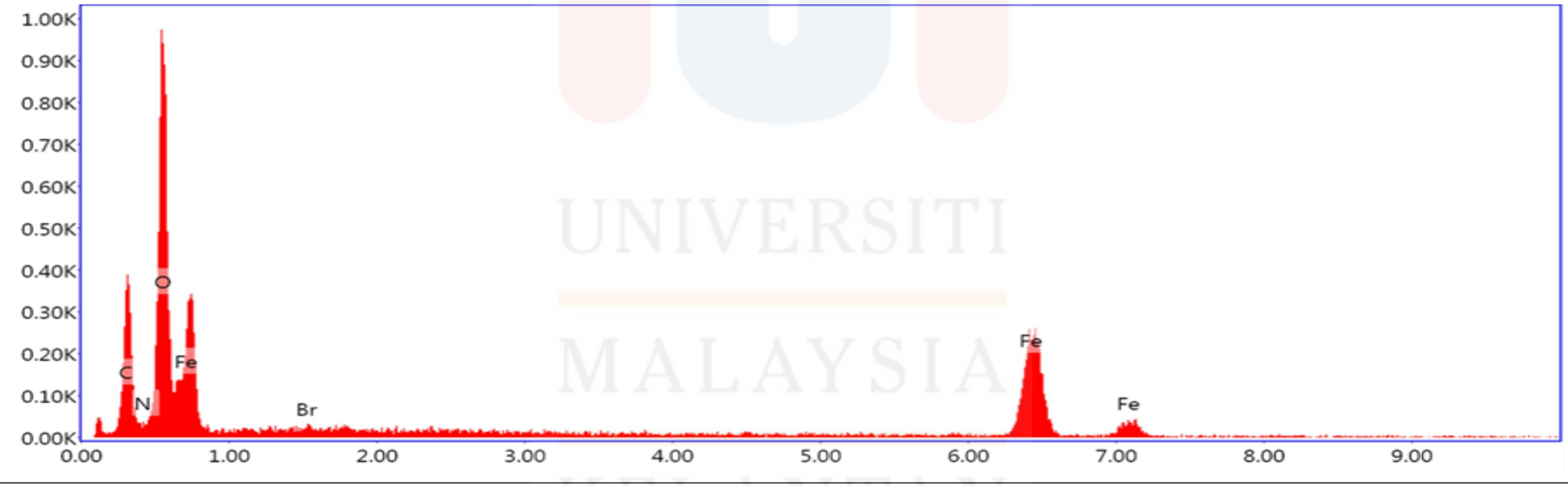

Figure 4.8.1: (c) The EDS spectra of MAC-CTAB.

d)

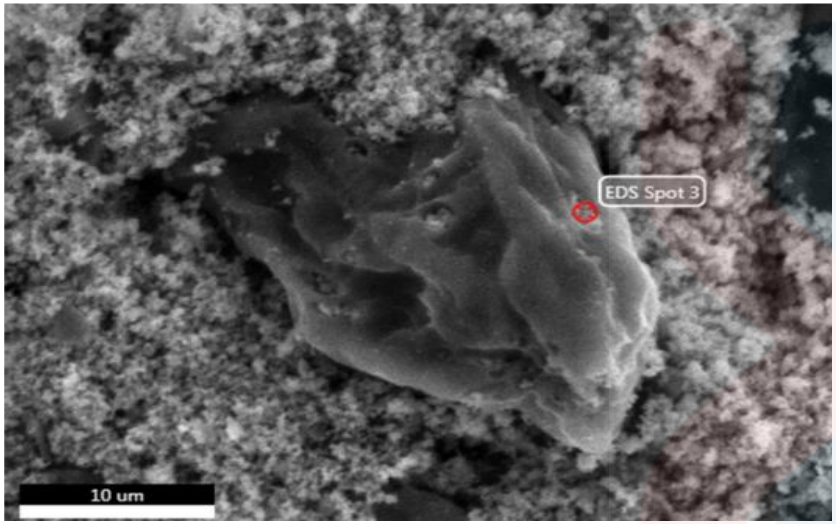

MAC-CPS		
Element	Weight (%)	Atomic (%)
C K	26.76	47.20
O K	25.53	33.31
SiK	2.39	1.80
FeK	45.32	17.19

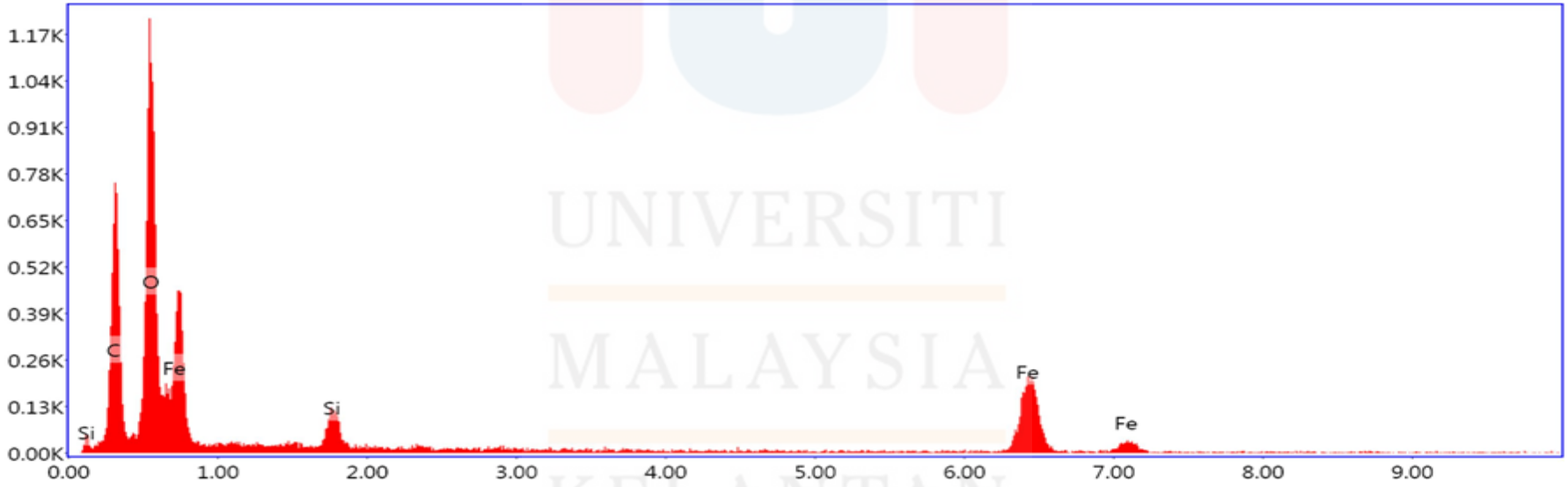

Figure 4.8.1: (d) The EDS spectra of MAC-CPS.

e)

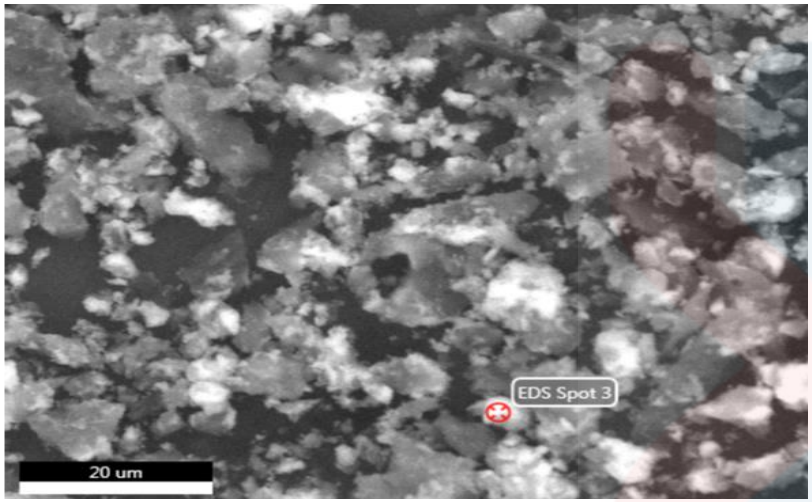

pMAC		
Element	Weight (%)	Atomic (%)
C K	34.52	52.78
O K	31.33	35.97
FeK	34.09	11.21

Figure 4.8.1: (e) The EDS spectra of pMAC.

Figure 4.8.1 (a) revealed that AC contained higher carbon content (88.84 %) followed by oxygen (10.99 %). For MAC, three main elements namely carbon, oxygen, and iron was indicated by spectrum. Iron was the highest of 66.31 % which was attributed to the iron oxide precipitated on the surface of AC during the magnetization process. The composition of oxygen (21.50 %) also increased with the iron. However, the composition of carbon found decrease in MAC compared to AC because of the coverage of iron oxide on its surface thus reduce the composition of carbon.

In Figure 4.8.1 (c), iron content was greatest of 63.62 % followed by oxygen (19.99 %) and carbon (11.72 %). The slightly decreased of iron content compared to MAC due to contained small amount (>5 %) of nitrogen and bromide composition which attributed to the CTAB cross-linked reaction. The presence of both elements might contributed to the incompletely distillation during preparation process thus resulted the contained of residual. Similar observation also found in Figure 4.8.1 (d) where iron content of MAC-CPS (45.32 %) was lower compared with MAC. This could be due to the smaller pore being selected for analysed thus affected the EDS spectrum of iron composition. The higher composition of oxygen among newly prepared MAC samples attributed to the oxide of silicon and iron. The exhibited of Si element (2.39 %) was demonstrated the existence of cross-linker agent.

Figure 4.8.1 (e) showed the spectrum contained three peaks which assigned to C, O, and Fe for pMAC in 34.52 %, 31.33 %, and 34.09 % respectively. The lower iron composition but highest in carbon elements compared to newly prepared MAC samples indicated the weak electrostatic force as well as magnetization presented in MB removal.

4.9 Thermogravimetric Analysis (TGA)

Thermogravimetric analysis is a technique used to analysis the weight changes of a sample as a function of temperature under a controlled atmosphere. Typical TGA curves of samples are depicted in Figure 4.9.1 at a starting temperature of 30 ℃ up to 980 ℃ while the temperature, percent weight loss and residual of samples after decomposition stage is summarize in Figure 4.9.1.

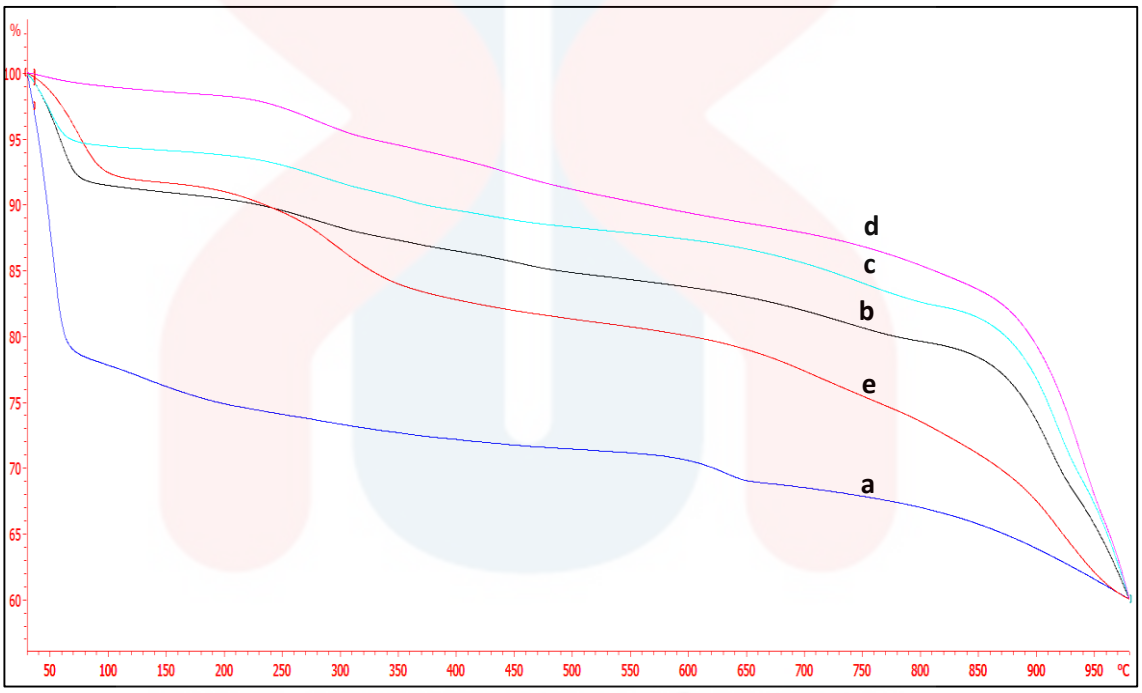

Figure 4.9.1: (a) Comparison of TGA patterns of AC, (b) MAC, (c) MAC-CTAB, (d) MAC-CPS, and (e) provided MAC.

Table 4.9.1: The percentage weight loss of samples at temperature up to 980 ℃.

Sample	Temperature (℃)	Weight loss (%)	Residual (%)
AC	42 - 528	13.63	86.33
	548-967	5.21	81.12
MAC (T_1)	42 - 483	7.11	92.88
	483 - 967	11.72	81.16
MAC-CTAB (T_2)	42 - 490	5.20	94.79
	490 - 967	12.55	82.24
MAC-CPS (T_3)	43 - 123	0.43	99.56
	123 - 492	2.69	96.87
	492 - 971	11.09	85.78
pMAC	42 - 167	8.54	91.46
	167 - 485	10.08	81.38
	485 - 969	21.37	60.01

The TGA curve of AC dramatically weight loss (13.63 %) at 42 to 548 ℃ accounts to evaporation of low volatile organic compounds, impurities and moisture (Verevkin, Ralys, Zaitsau, Emel'yanenko, & Schick, 2012). The slightly decreased of weight loss from 548 to 967 ℃ is accounts to intermediates further decomposition of AC. It was observed that 81.12 % residual of AC was lower than 81.16 % residual of MAC when temperature raised from 40 to 967 ℃. The slightly shifted to high residual suggesting that enhancement of thermal stability on iron oxide- loading AC.

From Table 4.9.1, MAC and MAC-CTAB exhibited two stages while MAC-CPS and pMAC were characterized by three different temperature stages. The weight loss of MAC-CPS (0.43 %) and pMAC (8.54 %) at first stage are attribute to the loss of moisture. The continuously decreased of both weight from 123 to 490 ℃ is the second stage as well as the first stage for MAC, and MAC-CTAB were suggest the chemical changes taking place and removal of labile oxygen-containing functional group (Kuila et al., 2012). It

was noted that all MAC samples begins to decompose around 490 ℃ due to the oxidation of carbon phase in magnetic composites (Xiao et al., 2013).

Figure 4.9.1 illustrates that MAC-CPS has higher thermal stability property among others as it can withstand extreme temperature. Besides, about 85.78 % of residual of Fe_2O_3 powder deposited on the surface of AC demonstrate that CPS suitable to use as cross-linking agent to enhance the stability of network of AC with magnetize powder. Overall thermal stability was as follows: MAC-CPS> MAC-CTAB> MAC> AC> pMAC.

4.10 Fourier Transform Infrared Spectroscopy (FTIR) Analysis

The prepared samples were characterized using FTIR spectroscopy (Thermo Scientific Nicolet iN10 Infrared Microscope & iZ10 FTIR module) to analyse the functional groups and changes in chemical composition of the mixture. The spectrum of prepared AC, MAC, MAC-CTAB, MAC-CPS, and pMAC are shown in Figure 4.10.1 in the range 500 - 4000 cm^{-1}.

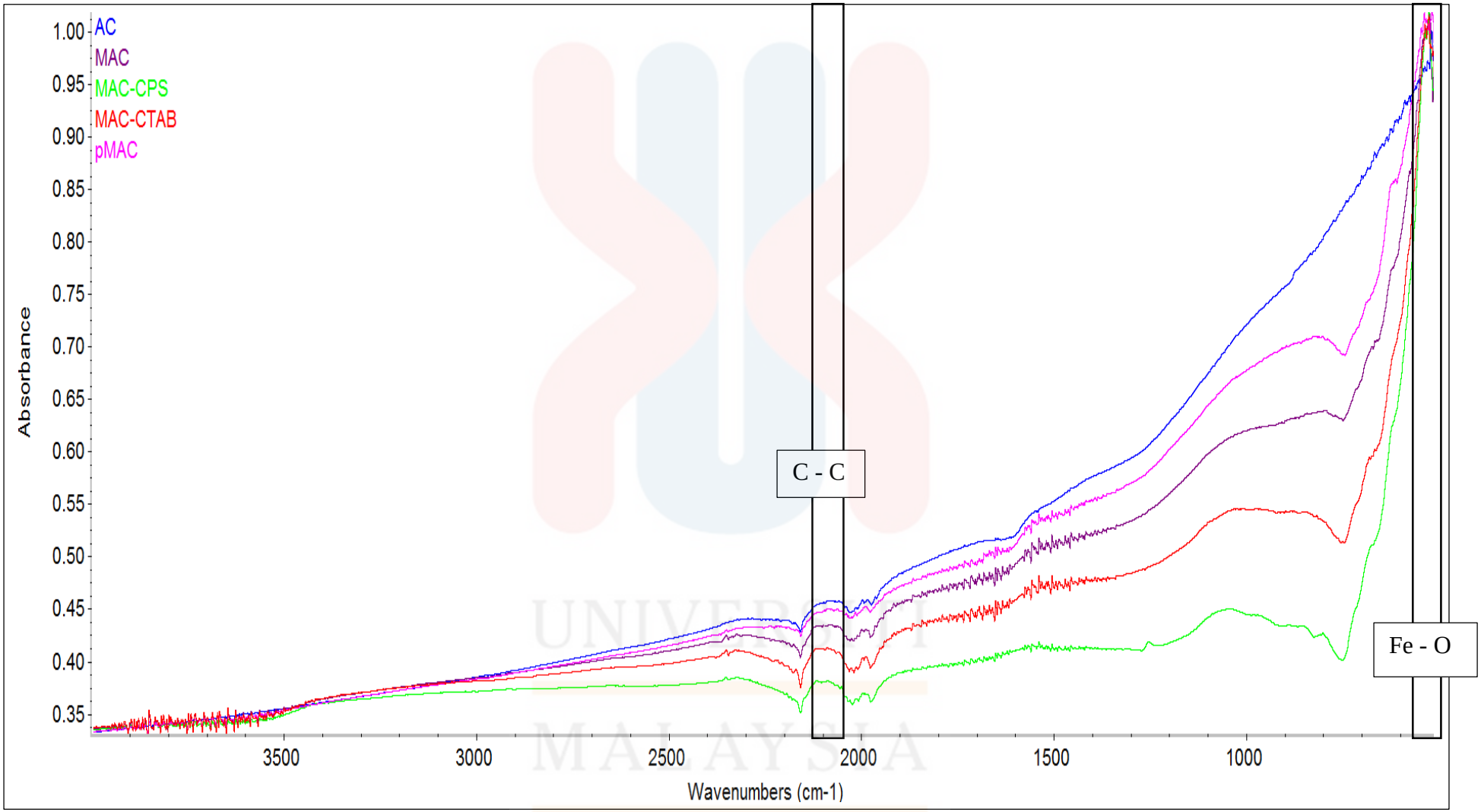

Figure 4.10.1: FTIR spectra of AC, MAC, MAC-CTAB, MAC-CPS, and provided MAC.

Table 4.10.1: Adsorption bands present in FTIR spectrum of AC, newly prepared MAC, MAC-CTAB, MAC-CPS, and pMAC.

Sample	Functional Group	Wave number (cm^{-1})
AC	C-C (stretching)	2075
MAC (T_1)	O-H (stretching)	3772
	C-C (stretching)	2080
	C=O (stretching)	1538
	Fe-O (stretching)	523
MAC-CTAB (T_2)	O-H (stretching)	3850
	C-C (stretching)	2088
	C=O (stretching)	1538
	Fe-O (stretching)	526
MAC-CPS (T_3)	O-H (stretching)	3667
	C-C (stretching)	2088
	C=O (stretching)	1539
	Si–O (stretching)	1254
	C-O (stretching)	1050
	Fe-O (stretching)	525
pMAC	O-H (stretching)	3799
	C-C (stretching)	2063
	C=O (stretching)	1538
	Fe-O (stretching)	537

The IR spectrum of AC showed only one band at 2075 cm^{-1} due to C-C stretching. After magnetization, the characteristic of MAC, MAC-CTAB, MAC-CPS, and pMAC

appeared a broad peak at 3580-3850 cm-^{1}, 2063-2088 cm-^{1}, 1538-1567 cm-^{1}, and 523-537 cm-^{1} correspond to O-H stretching (Yakout, & Sharaf El-Deen, 2016), C-C stretching, C=O stretching (V. K. Gupta, Agarwal, & Saleh, 2011), and Fe-O stretching (Lin et al., 2015) vibration, respectively. The peak at 523 cm-^{1} shifted to higher wavenumber (536 cm-^{1}) after the cross-linked reaction in MAC indicated the appearance of interaction between cross linker and MAC. Overall peaks are obviously weak in Figure 4.10.1.

It was noted that absorption peaks of MAC-CTAB shifted to higher wavenumber and amplitude after cross-linked reaction. According to Dobson, Roddick-Lanzilotta, & McQuillan (2000), peaks at 2920, 2855, or 1461 cm-^{1} would presence in the spectra if product contain CTAB residue. Hence, FTIR spectroscopic evidence revealed that cross-linked magnetic particles and AC by CTAB not obviously. In concomitance with the cross-linked CPS onto MAC, new peaks displayed at 1050 cm-^{1} correspond C-O stretching modes proposed the surface of MAC-CPS possesses oxygen-containing functional groups that providing reactive and anchoring sites to stabilize magnetic particles (Ai, Zhang, Liao, et al., 2011). Another new peak revealed the vibrational property of Si-C bond was observed at 1254 cm^{-1} which appointed to Si-C stretching (Tian et al., 2010)

4.11 X-ray diffraction (XRD) Analysis

The XRD diffractgram patterns of AC, MAC, cross-linked MACs, and pMAC was illustrated in Figure 4.11.1 to determine the crystalline properties on the samples.

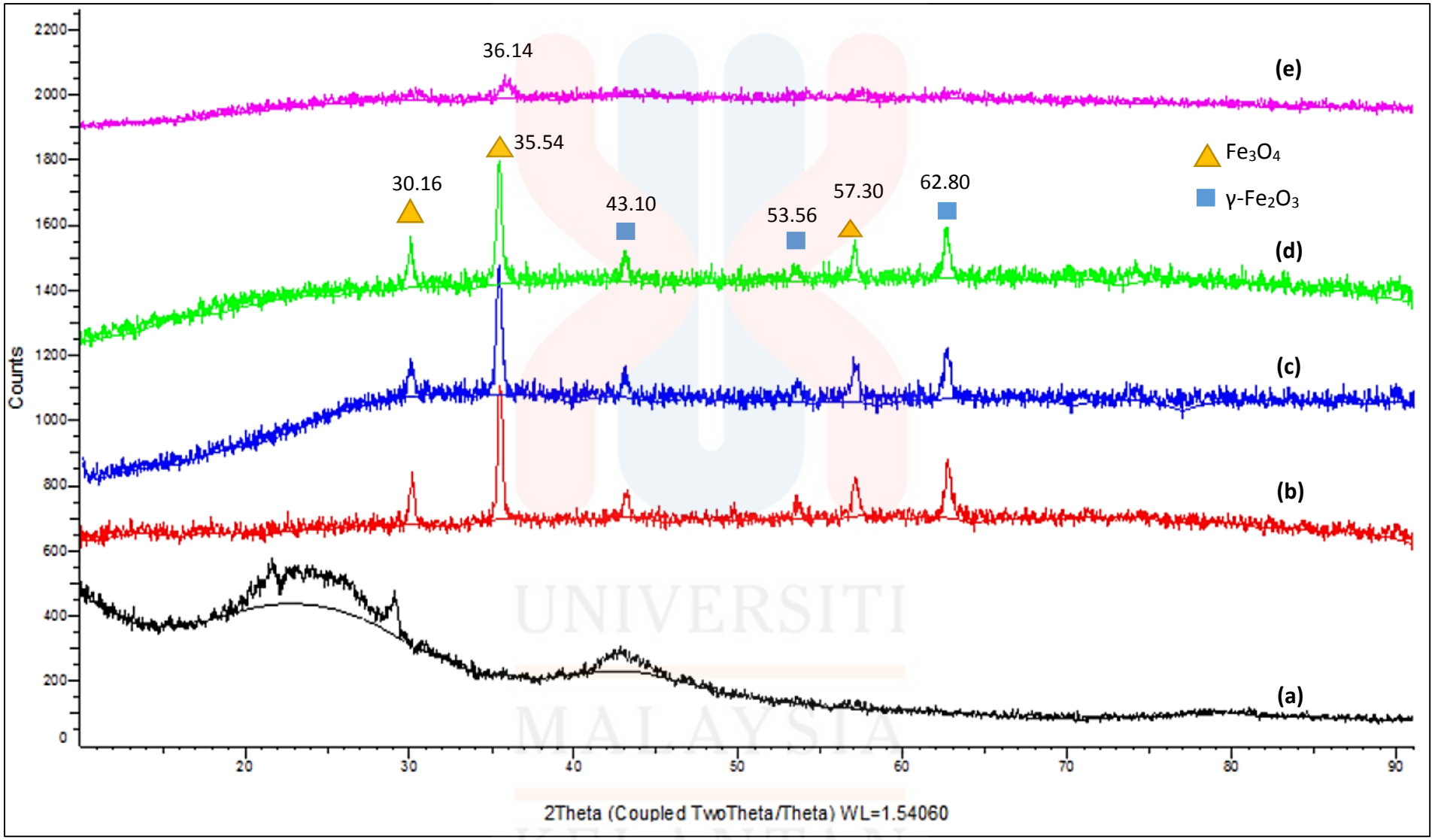

Figure 4.11.1: A comparison of the XRD patterns of (a) AC, (b) MAC, (c) MAC-CTAB, (d) MAC-CPS, and (e) pMAC.

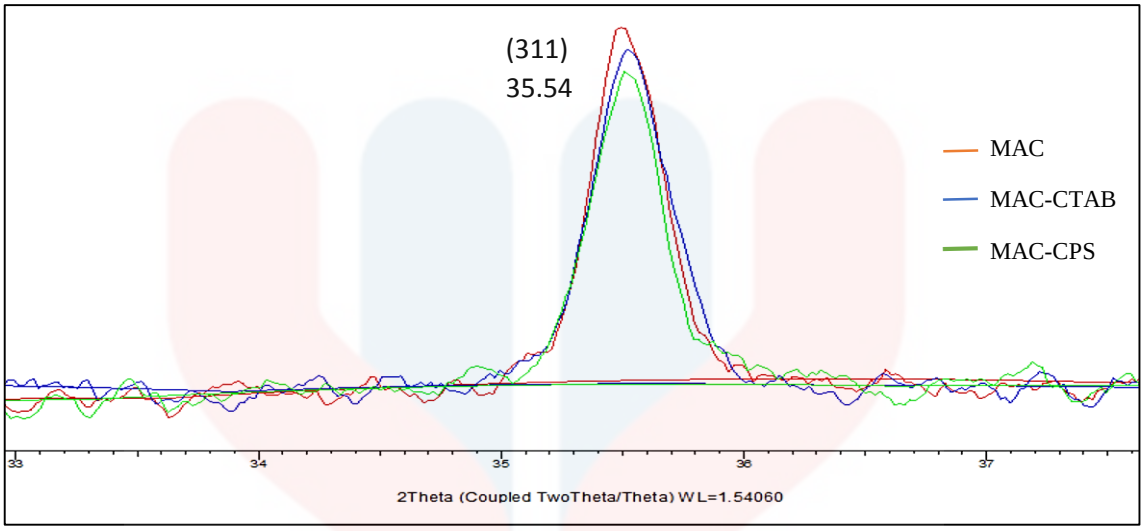

Figure 4.11.2: Magnified view of the X-ray diffraction patterns between 2θ of 33 °and 37 °.

As demonstrated in Figure 4.11.1, the predominantly amorphous structure of AC which absence of sharp peaks is advantageous property for well-defined adsorbents as well as precursor material (Boopathy, Karthikeyan, Mandal, and Sekaran, 2012). However, a peak can be observed at 2θ values of 29 ° may because of the presence of microcrystalline materials.

In addition, several peaks were obtained in newly prepared MAC samples due to the presence of crystalline phase of iron oxide in the porous AC. Three intense peaks displayed at 2θ values of 30.16 °, 35.54 °, and 57.30 ° assign as Fe_3O_4 (JCPDS-19-0629) and existence of γ-Fe_2O_3 peaks in accordance with JCPDS card (JCPDS-39-1346) at 43.10 °, 53.56 °, and 62.80 °for the newly prepared MACs. All the peaks correspond to the cubic indices (2 2 0), (3 1 1), (4 0 0), (4 2 2), (5 1 1), and (4 4 0) planes respectively. The crystalline patterns of the newly prepared MAC samples suggested the presence of γ-Fe_2O_3, Fe_3O_4 or both. Similar observation of XRD pattern was reported by Anyika, Asri,

Majid, Yahya, & Jaafar (2017) study in combination iron oxide with AC contained some peaks assigned to Fe_3O_4 and γ-Fe_2O_3.

To differentiate the phase, a portion of XRD data in 2θ regimes was expanded to figure the feature. As shown in Figure 4.11.2, it is noted that the line weight (311) have smaller 2θ value in the range between 35.00 °-36.00 °. Similar observation was reported by Bhagwat et al. (2007) that magnetite (35.00 °-36.00°) presented smaller 2θ value range than maghemite, γ-Fe_2O_3 (35.00 °-36.5 °). Thus, the newly prepared samples were supposed that reduced to magnetite Fe_3O_4. Meanwhile, the amorphous nature of pMAC showed in Figure 4.11.1 (e) presence 1 peak at 2θ = 36.14°

4.12 Precautions of Research

During lab work, some unexpected outcomes which resulted of mistakes in term of technical skills and external factor. These mistakes were recorded as reference for readers to avoid the same mistakes for similar research in future.

4.12.1 Inaccurate pH Adjustment

After the completion of cross-link reaction, MAC was washed with distilled water to adjust to pH 7. However, pH of solution showed inconsistent reading for every measurement as well as after calibration process. This happened possibly aberrant pH meter and make inaccurate pH testing of samples.

4.12.2 Rusted of Prepared MAC

Drying is needed after distillation process of MAC for standby to application. However, the MAC showed rusted after overnight drying and cannot use for further experiment. This happened might due to cross-contaminate reaction by samples of other people as the oven is public use. Thus, unknown chemical compound existence could possibly make the oxidation of MAC sample. The oxidize of MAC might contributed to the high moisture environment provided by oven.

Figure 4.12.2.1: Rusted (left) and ordinary MAC (right).

4.12.3 Inability in Producing MAC

In order to enhance the cross-link reaction in MAC, high temperature (85 ℃) was recommended during agitation process in MAC preparation. Since the maximum temperature and of orbital shaker incubator was limited at 70 ℃, therefore might resulted the incomplete inherent reaction between cross-linker and MAC. The incompletely of cross-link reaction contributed to the leaching behaviour of MAC and affect the adsorption ability in water treatment.

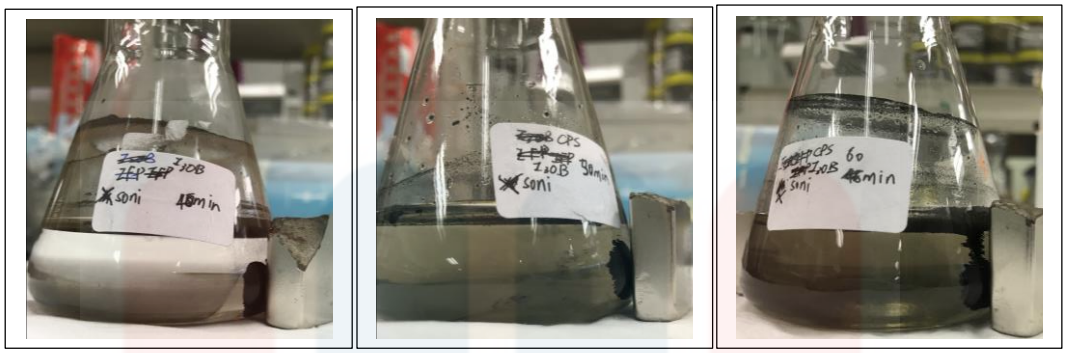

Figure 4.12.3.1: The MB removal by MAC showed a clear solution turned slightly cloudy followed by cloudiness yellow in 40, 50, and 60 min of shaking time (leaching behaviour of MAC).

4.12.4 Inaccurate Assay for Absorbance Reading

The MB solution after treated by AC was collected through filter paper filtration for absorbance reading. However, it was noted that the colour obtained in cuvette have a large different compared to the solution collected by pipette after sedimentation of AC. As Figure 4.12.4.1 showed, the overall colour of solution on upper side is clearer than solution on lower side which collected through filtration and pipette adsorption (after sedimentation was complete) respectively. This happened due to the surface of filter paper contained anionic surfactant which will adsorbed the cationic MB thus resulted a different absorbance reading of same solution.

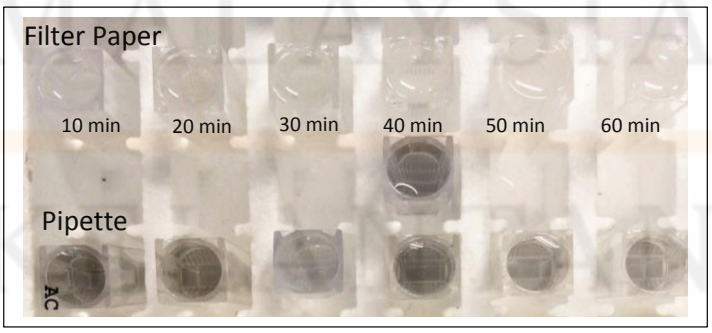

Figure 4.12.4.1: Solution collected through filter paper (above) and pipette (below).

4.13 Suggestion for Improved Experiment

Based on the research, there were some recommendation or suggestion that may be able to improve the experiment in order to get the better results. Technical recommendation was valuable to act as reference for future researches in lab scale.

4.13.1 Sieving of Samples

The newly prepared MAC attributed different particles size after drying process which could affect the preciseness of sample as well as adsorption capacity. Thus, it was recommended to sieve again after the drying process to avoid the inconsistence particle size used.

4.13.2 pH Adjustment Skills

It was recommended to leave the solution for a while after pH adjustment for pH stabilization. Then, checking on solution pH was carried out again for accurate pH value. Next, diluted acid or base was used instead of absolute concentration to avoid vigorous chemical reaction.

4.13.3 Sufficient Agitation

Based on observation, the hydrophobic composition required longer time and higher agitation for stirring. Hence, sufficient agitation should be ensuring for effective cross-linked reaction by well stirring of solution especially magnetization and cross-link processes. Figure below with red mark shown floating of CPS at top of solution which resulting insufficient agitation.

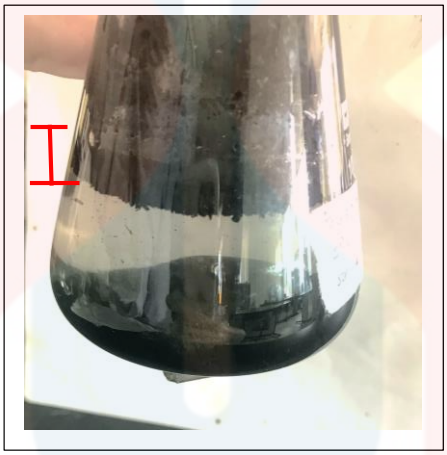

Figure 4.13.3.1: Floating of CPS chemical on the surface of solution.

4.13.4 Equal Solution Volume in Cuvette

Spectrophotometry is a method to measure how much a chemical substance absorbs light by measuring the intensity of light as a beam of light passes through sample solution. Therefore, every solution for undergo absorbance reading should at a same level in cuvette since high volume of solvent will always have more “free” particles inside and contributed inconsistent absorbance reading.

CHAPTER 5

CONCLUSION AND RECOMMENDATION

5.1 Conclusion

As the conclusion of this research, all the objectives were accomplished successfully. The cross-linked iron oxide particle and AC by CTAB and CPS showed excellent paramagnetic properties as they could be effectively separated from solution. MAC-CPS presented the greatest follow by MAC, MAC-CTAB, AC, and pMAC in term of effectiveness for MB removal. This illustrated that presence of cross-linked enhance the MB removal ability. The characterizations results indicated that cross-linked agent altered the properties of MAC. In iodine test, cross-linked MACs showed different result. The porous volume decreases compare to MAC and AC. Low porous volume with high removal efficiency suggest that electrostatic attraction was the dominant mechanisms for the sorption of MB onto the MAC-CPS. Whereas MAC cross-linked with CTAB did not affect the pore structure of MAC. The FTIR spectrum obtained for MAC was observed to be similar to spectrum of cross-linked MAC. XRD data suggest that the main magnetic

phase formed in the newly prepared MAC is magnetite, possibly with small amounts of maghemite. This supports that the newly prepared MAC samples have the potential to become excellent adsorbent attributable to the strong magnetic property. SEM images of both cross-linked agents showed that the reducing porosity on the surface after cross-linked reaction. Fe, C, and O assigned as main compositions obtained in MAC samples. In TGA analysis, both the CTAB and CPS cross-linked MAC demonstrated high ability to withstand high temperature and significantly stable property compared to MAC. Overall, MB removal efficiency from MAC-CPS was higher than that of MAC-CTAB. This research could serve as a step towards further investigation on the optimization of method and condition in magnetic properties, sorption study for synthesis magnetic biocarbon by using CPS, as well as act as reference for other cross-link reaction.

5.2 Recommendation

For recommendation in aspect of further study in future prospects, some technical recommendation have been mentioned previously at Chapter 4.13. Besides the technical recommendation, research more information is recommending before carrying out any experiments to avoid unnecessary troubles. It was an individually and independently project. Mistakes happened during the research due to lack of experience and understanding. However, mistakes made perfect. It's so called research as requirement of searching again and again. I would like to encourage the readers not to give up when encountering any obstacles. Developing a positive attitude in any circumstances is important for personality. As conclusion, Final Year Project (FYP) was actually a learning process.

References

Ai, L., Zhang, C., Liao, F., Wang, Y., Li, M., Meng, L., & Jiang, J. (2011). Removal of methylene blue from aqueous solution with magnetite loaded multi-wall carbon nanotube: Kinetic, isotherm and mechanism analysis. *Journal of Hazardous Materials*, *198*, 282–290. https://doi.org/10.1016/j.jhazmat.2011.10.041

ASTM D4607- 94. (2006). Standard Test Method for Determination of Iodine Number of Activated Carbon 1. *ASTM International*, *94*(Reapproved), 1–5. https://doi.org/10.1520/D4607-14.2

Ahmad, M., Lee, S. S., Dou, X., Mohan, D., Sung, J.-K., Yang, J. E., & Ok, Y. S. (2012). Effects of pyrolysis temperature on soybean stover- and peanut shell-derived biochar properties and TCE adsorption in water. *Bioresource Technology*, *118*, 536–544. https://doi.10.1016/j.biortech.2012.05.042

Alhassani, H., Rauf, M., & Ashraf, S. (2007). Efficient microbial degradation of Toluidine Blue dye by Brevibacillus sp. *Dyes and Pigments*, *75*(2), 395–400. https://doi.10.1016/j.dyepig.2006.06.019

Altıntıg, E., Altundag, H., Tuzen, M., & Sarı, A. (2017). Effective removal of methylene blue from aqueous solutions using magnetic loaded activated carbon as novel adsorbent. *Chemical Engineering Research and Design*, *122*, 151–163. https://doi.10.1016/j.cherd.2017.03.035

Anyika, C., Asri, N. A. M., Majid, Z. A., Yahya, A., & Jaafar, J. (2017). Synthesis and characterization of magnetic activated carbon developed from palm kernel shells. *Nanotechnology for Environmental Engineering*, *2*(1), 16. https://doi.org/10.1007/s41204-017-0027-6

Beesley, L., Moreno-Jiménez, E., Gomez-Eyles, J. L., Harris, E., Robinson, B., & Sizmur, T. (2011). A review of biochars' potential role in the remediation, revegetation and restoration of contaminated soils. *Environmental Pollution*, *159*(12), 3269–3282. https://doi.10.1016/j.envpol.2011.07.023

Ben Mansour, H., Houas, I., Montassar, F., Ghedira, K., Barillier, D., Mosrati, R., & Chekir-Ghedira, L. (2012). Alteration of in vitro and acute in vivo toxicity of textile dyeing wastewater after chemical and biological remediation. *Environmental Science and Pollution Research*, *19*(7), 2634–2643. https://doi.10.1007/s11356-012-0802-7

Bhagwat. S., Singh, H., Athawale, A., Hannoyer, B., Jouen, S., Lefez, B., Kundaliya, D., & Ogale, S. (2007). Low Temperature Synthesis of Magnetite and Maghemite Nanoparticles. *Journal of Nanoscience and Nanotechnology*, *7*, 4294–4302. https:// doi.10.1166/jnn.2007.873

Bilal, M., Asgher, M., Iqbal, H. M. N., Hu, H., & Zhang, X. (2017). Bio-based degradation of emerging endocrine-disrupting and dye-based pollutants using

cross-linked enzyme aggregates. *Environmental Science and Pollution Research, 24*(8), 7035–7041. https://doi.10.1007/s11356-017-8369-y

Boopathy, R., Karthikeyan, S., Mandal, A. B., & Sekaran, G. (2012). Adsorption of ammonium ion by coconut shell-activated carbon from aqueous solution: kinetic, isotherm, and thermodynamic studies. *Environmental Science and Pollution Research, 20*(1), 533–542. https://doi.10.1007/s11356-012-0911-3

Bouyakoub, A. Z., Lartiges, B. S., Ouhib, R., Kacha, S., El Samrani, A. G., Ghanbaja, J., & Barres, O. (2011). MnCl2 and MgCl2 for the removal of reactive dye Levafix Brilliant Blue EBRA from synthetic textile wastewaters: An adsorption/aggregation mechanism. *Journal of Hazardous Materials, 187*(1-3), 264–273. https://doi.10.1016/j.jhazmat.2011.01.008

Cazetta, A. L., Vargas, A. M. M., Nogami, E. M., Kunita, M. H., Guilherme, M. R., Martins, A. C., … Almeida, V. C. (2011). NaOH-activated carbon of high surface area produced from coconut shell: Kinetics and equilibrium studies from the methylene blue adsorption. *Chemical Engineering Journal*, *174*(1), 117–125. https://doi.org/10.1016/j.cej.2011.08.058

Chakraborty, S., De, S., DasGupta, S., & Basu, J. K. (2005). Adsorption study for the removal of a basic dye: experimental and modeling. *Chemosphere*, *58*(8), 1079–1086. http://doi.10.1016/j.chemosphere.2004.09.066

Chen, C., Hu, J., Shao, D., Li, J., & Wang, X. (2009). Adsorption behaviour of multiwall carbon nanotube/iron oxide magnetic composites for Ni(II) and Sr(II). *Journal of Hazardous Materials*, *164*(2-3), 923–928. https://doi.10.1016/j.jhazmat.2008.08.089

Dawood, S., & Sen, T. K. (2012). Removal of anionic dye Congo red from aqueous solution by raw pine and acid-treated pine cone powder as adsorbent: Equilibrium, thermodynamic, kinetics, mechanism and process design. *Water Research, 46*(6), 1933–1946. https://doi.10.1016/j.watres.2012.01.009

Dekant, W., & Klaunig, J. E. (2016). Toxicology of decamethylcyclopentasiloxane (D5). Regulatory *Toxicology and Pharmacology*, *74*, S67–S76. https://doi.10.1016/j.yrtph.2015.06.011

Dias, J. M., Alvim-Ferraz, M. C. M., Almeida, M. F., Rivera-Utrilla, J., & Sánchez-Polo, M. (2007). Waste materials for activated carbon preparation and its use in aqueous-phase treatment: A review. *Journal of Environmental Management*, *85*(4), 833–846. https://doi.org/10.1016/j.jenvman.2007.07.031

Dobson, K. D., Roddick-Lanzilotta, A. D., & McQuillan, A. J. (2000). An in situ infrared spectroscopic investigation of adsorption of sodium dodecylsulfate and of cetyltrimethylammonium bromide surfactants to TiO2, ZrO2, Al2O3, and Ta2O5

particle films from aqueous solutions. *Vibrational Spectroscopy, 24*(2), 287–295. https://doi.10.1016/s0924-2031(00)00096-5

Donia, A. M., Atia, A. A., & Elwakeel, K. Z. (2008). Selective separation of mercury(II) using magnetic chitosan resin modified with Schiff's base derived from thiourea and glutaraldehyde. *Journal of Hazardous Materials, 151*(2-3), 372–379. https://doi:10.1016/j.jhazmat.2007.05.083

Garc á, J. R., Sedran, U., Zaini, M. A. A., & Zakaria, Z. A. (2017). Preparation, characterization, and dye removal study of activated carbon prepared from palm kernel shell. *Environmental Science and Pollution Research, 25*(6), 5076–5085. https://doi.10.1007/s11356-017-8975-8

Ghasemian Lemraski, E., Sharafinia, S., & Alimohammadi, M. (2017). New Activated Carbon from Persian Mesquite Grain as an Excellent Adsorbent. *Physical and Chemical Resources, 5*(1), 81-98. https://doi.10.22036/PCR.2017.38495

Gong, J.L., Wang, B., Zeng, G.M., Yang, C.P., Niu, C.G., Niu, Q.Y., … Liang, Y. (2009). Removal of cationic dyes from aqueous solution using magnetic multi-wall carbon nanotube nanocomposite as adsorbent. *Journal of Hazardous Materials, 164*(2-3), 1517–1522. https://doi.org/10.1016/j.jhazmat.2008.09.072

Graf, C., Vossen, D. L. J., Imhof, A., & van Blaaderen, A. (2003). A General Method To Coat Colloidal Particles with Silica. *Langmuir, 19*(17), 6693–6700. https://doi.10.1021/la0347859

Gratuito, M. K. B., Panyathanmaporn, T., Chumnanklang, R. A., Sirinuntawittaya, N., & Dutta, A. (2008). Production of activated carbon from coconut shell: Optimization using response surface methodology. *Bioresource Technology*, *99*(11), 4887–4895. https://doi.org/10.1016/j.biortech.2007.09.042

Gupta, V. K., Agarwal, S., & Saleh, T. A. (2011). Chromium removal by combining the magnetic properties of iron oxide with adsorption properties of carbon nanotubes. *Water Research*, *45*(6), 2207–2212. https://doi.org/10.1016/j.watres.2011.01.012

Gupta, V. K., Mittal, A., Kurup, L., & Mittal, J. (2006). Adsorption of a hazardous dye, erythrosine, over hen feathers. *Journal of Colloid and Interface Science*, *304*(1), 52–57. http://doi.10.1016/j.jcis.2006.08.032

Gurses, A., Yalcin, M., Sozbilir, M., & Dogar, C. (2003). The investigation of adsorption thermodynamics and mechanism of a cationic surfactant, CTAB, onto powdered active carbon. *Fuel Processing Technology, 81*(1), 57–66. https://doi.10.1016/s0378-3820(03)00002-x

Gwenzi, W., Chaukura, N., Noubactep, C., & Mukome, F. N. D. (2017). Biochar-based water treatment systems as a potential low-cost and sustainable technology for clean water provision. *Journal of Environmental Management*, *197*, 732–749. https://doi.10.1016/j.jenvman.2017.03.087

Hakam A, Rahman IA, Jamil MSM, Othaman R, Amin MCIM, Lazim AM (2015) Removal of methylene blue dye in aqueous solution by sorption on a bacterial-g-poly- (acrylic acid) polymer network hydrogel. *Sains Malaysiana 44*:827–834. https://doi.org/10.17576/jsm2015-4406-08

Hale, S. E., Lehmann, J., Rutherford, D., Zimmerman, A. R., Bachmann, R. T., Shitumbanuma, V., … Cornelissen, G. (2012). Quantifying the Total and Bioavailable Polycyclic Aromatic Hydrocarbons and Dioxins in Biochars. *Environmental Science & Technology, 46*(5), 2830–2838.

Hu, X., Wang, J., Liu, Y., Li, X., Zeng, G., Bao, Z., … Long, F. (2011). Adsorption of chromium (VI) by ethylenediamine-modified cross-linked magnetic chitosan resin: Isotherms, kinetics and thermodynamics. *Journal of Hazardous Materials, 185*(1), 306–314. https://doi:10.1016/j.jhazmat.2010.09.034

Illert, P., Wängler, B., Wängler, C., & Röder, T. (2017). Size-controllable synthesis of polymeric iodine-carrying nanoparticles for medical CT imaging. *Polymers for Advanced Technologies, 28*(12), 1610–1616. https://doi.10.1002/pat.4043

Inyang, M., & Dickenson, E. (2015). The potential role of biochar in the removal of organic and microbial contaminants from potable and reuse water: A review. *Chemosphere, 134*, 232–240. https://doi.10.1016/j.chemosphere.2015.03.072

Jan, S. & Hasal, P. (2013). Photocatalytic Degradation of Textile Dyes in Atio (2)/UV System. 11Th International Conference On *Chemical and Process Engineering 32:* 79-84. https://doi.10.3303/CET1332014.

Kallel, F., Bouaziz, F., Chaari, F., Belghith, L., Ghorbel, R., & Chaabouni, S. E. (2016). Interactive effect of garlic straw on the sorption and desorption of Direct Red 80 from aqueous solution. *Process Safety and Environmental Protection, 102*, 30–43. https://doi.10.1016/j.psep.2016.02.012

Katheresan, V., Kansedo, J., & Lau, S. Y. (2018). Efficiency of various recent wastewater dye removal methods: A review. *Journal of Environmental Chemical Engineering, 6*(4), 4676–4697. https://doi.10.1016/j.jece.2018.06.060

Kavitha, D., & Namasivayam, C. (2007). Experimental and kinetic studies on methylene blue adsorption by coir pith carbon. *Bioresource Technology, 98*(1), 14–21. https://doi:10.1016/j.biortech.2005.12.008

Khayet, M., Zahrim, A. Y., & Hilal, N. (2011). Modelling and optimization of coagulation of highly concentrated industrial grade leather dye by response surface methodology. *Chemical Engineering Journal, 167*(1), 77–83. https://doi.10.1016/j.cej.2010.11.108

Khouni, I., Marrot, B., Moulin, P., & Ben Amar, R. (2011). Decolourization of the reconstituted textile effluent by different process treatments: Enzymatic catalysis, coagulation/flocculation and nanofiltration processes. *Desalination, 268*(1-3), 27–37. https://doi:10.1016/j.desal.2010.09.046

Kousha, M., Daneshvar, E., Esmaeli, A. R., Jokar, M., & Khataee, A. R. (2012). Optimization of Acid Blue 25 removal from aqueous solutions by raw, esterified and protonated Jania adhaerens biomass. *International Biodeterioration & Biodegradation, 69*, 97–105. https://doi.10.1016/j.ibiod.2012.01.007

Kuila, T., Bose, S., Khanra, P., Mishra, A. K., Kim, N. H., & Lee, J. H. (2012). A green approach for the reduction of graphene oxide by wild carrot root. *Carbon, 50* (3), 914–921. https://doi.10.1016/j.carbon.2011.09.053

Lachheb, H., Puzenat, E., Houas, A., Ksibi, M., Elaloui, E., Guillard, C., & Herrmann, J.-M. (2002). Photocatalytic degradation of various types of dyes (Alizarin S, Crocein Orange G, Methyl Red, Congo Red, Methylene Blue) in water by UV-irradiated titania. *Applied Catalysis B: Environmental, 39*(1), 75–90. https://doi.10.1016/s0926-3373(02)00078-4

Lade, H. S., Waghmode, T. R., Kadam, A. A., & Govindwar, S. P. (2012). Enhanced biodegradation and detoxification of disperse azo dye Rubine GFL and textile industry effluent by defined fungal-bacterial consortium. *International Biodeterioration & Biodegradation, 72*, 94–107. https://doi.10.1016/j.ibiod.2012.06.001

Laksaci, H., Khelifi, A., Trari, M., & Addoun, A. (2017). Synthesis and characterization of microporous activated carbon from coffee grounds using potassium hydroxides. *Journal of Cleaner Production, 147*, 254–262. https://doi.10.1016/j.jclepro.2017.01.102

Lin, Q., Liu, X., He, Y., Huang, H., & Shen, X. (2015). Spin-Glass Behavior, Magnetic, and IR Spectroscopy Analysis of Multimetallic Compound Ni0.25Mn1.25[Fe(CN)6] 6.1H2O. *Journal of Spectroscopy*, 2015, 1–6. http://doi:10.1155/2015/385215

Liu, X., Marangon, I., Melinte, G., Wilhelm, C., Ménard-Moyon, C., Pichon, B. P., … Bégin, D. (2014). Design of Covalently Functionalized Carbon Nanotubes Filled with Metal Oxide Nanoparticles for Imaging, Therapy, and Magnetic Manipulation. *ACS Nano, 8*(11), 11290–11304. https://doi.10.1021/nn5040923

Luo, X., & Zhang, L. (2009). High effective adsorption of organic dyes on magnetic cellulose beads entrapping activated carbon. *Journal of Hazardous Materials, 171*(1-3), 340–347. https://doi.10.1016/j.jhazmat.2009.06.009

Manju, A., & Bishnoi, N. (2016). Adsorption of Methylene Blue On Spent Immobilized Biomass of Rice Straw Left After Enzyme Production. *International Journal of Advanced Multidisciplinary Research (IJAMR) 3* (7): 12-18.

Merzouk, B., Gourich, B., Madani, K., Vial, C., & Sekki, A. (2011). Removal of a disperse red dye from synthetic wastewater by chemical coagulation and continuous electrocoagulation. A comparative study. *Desalination, 272*(1-3), 246–253. https://doi:10.1016/j.desal.2011.01.029

Mirimin, L., & Roodt-Wilding, R. (2015). Testing and validating a modified CTAB DNA extraction method to enable molecular parentage analysis of fertilized eggs and larvae of an emerging South African aquaculture species, the dusky kobArgyrosomus japonicus. *Journal of Fish Biology, 86*(3), 1218–1223. https://doi.10.1111/jfb.12639

Mohamed, M. M. (2004). Acid dye removal: comparison of surfactant-modified mesoporous FSM-16 with activated carbon derived from rice husk. *Journal of Colloid and Interface Science, 272*(1), 28–34. https://doi.10.1016/j.jcis.2003.08.071

Mohan, D., Sarswat, A., Ok, Y. S., & Pittman, C. U. (2014). Organic and inorganic contaminants removal from water with biochar, a renewable, low cost and sustainable adsorbent - A critical review. *Bioresource Technology*, *160*, 191–202. https://doi.org/10.1016/j.biortech.2014.01.120

Mudyawabikwa, B., Mungondori, H. H., Tichagwa, L., & Katwire, D. M. (2017). Methylene blue removal using a low-cost activated carbon adsorbent from tobacco stems: kinetic and equilibrium studies. *Water Science and Technology*, 75(10), 2390–2402. https://doi.10.2166/wst.2017.041

Munoz, M., de Pedro, Z. M., Casas, J. A., & Rodriguez, J. J. (2015). Preparation of magnetite-based catalysts and their application in heterogeneous Fenton oxidation – A review. *Applied Catalysis B: Environmental*, *176*, 249–265. https://doi.10.1016/j.apcatb.2015.04.003

Nadeem, M., Mahmood, A., Shahid, S. A., Shah, S. S., Khalid, A. M., & Mckay, G. (2006). Sorption of lead from aqueous solution by chemically modified carbon adsorbents, *138*, 604–613. https://doi.org/10.1016/j.jhazmat.2006.05.098

Namasivayam, C., & Kavitha, D. (2002). Removal of Congo Red from water by adsorption onto activated carbon prepared from coir pith, an agricultural solid waste Removal of Congo Red from water by adsorption onto activated carbon prepared from coir pith, *54*(July 2015), 47–58. https://doi.org/10.1016/S0143-7208(02)00025-6

Namduri, H., & Nasrazadani, S. (2008). Quantitative analysis of iron oxides using Fourier transform infrared spectrophotometry. *Corrosion Science*, *50*(9), 2493–2497. https://doi.org/10.1016/j.corsci.2008.06.034

Nataraj, S. K., Hosamani, K. M., & Aminabhavi, T. M. (2009). Nanofiltration and reverse osmosis thin film composite membrane module for the removal of dye and salts from the simulated mixtures. *Desalination, 249*(1), 12–17. https://doi.10.1016/j.desal.2009.06.008

Oliveira, L. C. A., Rios, R. V. R. A., Fabris, J. D., Garg, V., Sapag, K., & Lago, R. M. (2002). Activated carbon/iron oxide magnetic composites for the adsorption of

contaminants in water. *Carbon, 40(12),* 2177–2183. https://doi.10.1016/s0008-6223(02)00076-3

Oz, M., Lorke, D. E., Hasan, M., & Petroianu, G. A. (2010). Cellular and molecular actions of Methylene Blue in the nervous system. *Medicinal Research Reviews, 31*(1), 93–117. https://doi.10.1002/med.20177

Pillay, K., Cukrowska, E. M., & Coville, N. J. (2009). Multi-walled carbon nanotubes as adsorbents for the removal of parts per billion levels of hexavalent chromium from aqueous solution. *Journal of Hazardous Materials, 166(2-3),* 1067–1075. https://doi.10.1016/j.jhazmat.2008.12.011

Rafatullah, M., Sulaiman, O., Hashim, R., & Ahmad, A. (2010). Adsorption of methylene blue on low-cost adsorbents: A review. *Journal of Hazardous Materials*, *177*(1–3), 70–80. https://doi.org/10.1016/j.jhazmat.2009.12.047

Rodr ́guez-Couto, S., Osma, J. F., & Toca-Herrera, J. L. (2009). Removal of synthetic dyes by an eco-friendly strategy. *Engineering in Life Sciences, 9*(2), 116–123. https://doi.10.1002/elsc.200800088

Robinson, T., McMullan, G., Marchant, R., & Nigam, P. (2001). Remediation of dyes in textile effluent: a critical review on current treatment technologies with a proposed alternative. *Bioresource Technology, 77*(3), 247–255. https://doi.10.1016/s0960-8524(00)00080-8

Šćiban, M., Klašnja, M., & Škrbić, B. (2008). Adsorption of copper ions from water by modified agricultural by-products. *Desalination, 229*(1-3), 170–180. https://doi.10.1016/j.desal.2007.08.017

Sen, T. K., Afroze, S., & Ang, H. M. (2010). Equilibrium, Kinetics and Mechanism of Removal of Methylene Blue from Aqueous Solution by Adsorption onto Pine Cone Biomass of Pinus radiata. *Water, Air, & Soil Pollution, 218*(1-4), 499–515. https://doi.10.1007/s11270-010-0663-y

Sharma, R. K., Puri, A., Kumar, A., Monga, Y., Gaba, G., & Adholeya, A. (2014). Diacetylmonoxime Functionalized Silica Gel: An Efficient and Recyclable Organic Inorganic Hybrid Material for Selective Removal of Copper from Fly Ash Ameliorated Soil Samples. *Separation Science and Technology, 49*(5), 709–720. https://doi:10.1080/01496395.2013.853678

Singh, K., & Arora, S. (2011). Removal of Synthetic Textile Dyes From Wastewaters: A Critical Review on Present Treatment Technologies. *Critical Reviews in Environmental Science and Technology, 41*(9), 807–878. https://doi.10.1080/10643380903218376

Sivakumar, B., Kannan, C., & Karthikeyan, S. (2012). Preparation and characterization of activated carbon prepared from Balsamodendron caudatum wood waste through various activation processes. *Rasayan Journal of Chemistry*, *5*(3), 321–327.

Soon, A. N., & Hameed, B. H. (2011). Heterogeneous catalytic treatment of synthetic dyes in aqueous media using Fenton and photo-assisted Fenton process. *Desalination, 269*(1-3), 1–16. https://doi.10.1016/j.desal.2010.11.002

Strachowski, P., Kaszuwara, W., & Bystrzejewski, M. (2017). A novel magnetic composite adsorbent of phenolic compounds based on waste poly(ethylene terephthalate) and carbon-encapsulated magnetic nanoparticles. *New J. Chem., 41*(21), 12617–12630. https://doi.org/10.1039/C7NJ01818E

Suteu, D., Bilba, D., & Coseri, S. (2013). Macroporous polymeric ion exchangers as adsorbents for the removal of cationic dye basic blue 9 from aqueous solutions. *Journal of Applied Polymer Science, 131*(1), n/a–n/a. https://doi.10.1002/app.39620

Teow, Y. H., Nordin, N. I., & Mohammad, A. W. (2018). Green synthesis of palm oil mill effluent-based graphenic adsorbent for the treatment of dye-contaminated wastewater. *Environmental Science and Pollution Research*. https://doi:10.1007/s11356-018-2189-6

Tian, R., Seitz, O., Li, M., Hu, W. (Walter), Chabal, Y. J., & Gao, J. (2010). Infrared Characterization of Interfacial Si−O Bond Formation on Silanized Flat SiO2/Si Surfaces. *Langmuir, 26*(7), 4563–4566. https://doi.10.1021/la904597c

Tsai, W.T., Hsien, K.J., & Hsu, H.C. (2009). Adsorption of organic compounds from aqueous solution onto the synthesized zeolite. *Journal of Hazardous Materials, 166*(2-3), 635–641. https://doi.10.1016/j.jhazmat.2008.11.071

Verevkin, S. P., Ralys, R. V., Zaitsau, D. H., Emel'yanenko, V. N., & Schick, C. (2012). Express thermo-gravimetric method for the vaporization enthalpies appraisal for very low volatile molecular and ionic compounds. *Thermochimica Acta, 538*, 55–62. https://doi:10.1016/j.tca.2012.03.018

Verheijen, F. G. A., Jeffery, S., Bastos, A. C., Van der Velde, M., & Diafas, I. (2010). Biochar application to soils e a critical scientific review of effects on soil properties, processes and functions. EUR 24099 EN. Office for the Official Publications of the European Communities, Luxembourg.

Wong, S., Yac'cob, N. A. N., Ngadi, N., Hassan, O., & Inuwa, I. M. (2018). From pollutant to solution of wastewater pollution: Synthesis of activated carbon from textile sludge for dye adsorption. *Chinese Journal of Chemical Engineering, 26*(4), 870–878. https://doi.10.1016/j.cjche.2017.07.015

Wong, Y. C., Szeto, Y. S., Cheung, W. H., & McKay, G. (2004). Adsorption of acid dyes on chitosan—equilibrium isotherm analyses. *Process Biochemistry, 39*(6), 695–704. https://doi:10.1016/s0032-9592(03)00152-3

Worch, E. (2012). *Adsorption Technology in Water Treatment: Fundamentals, Processes, and Modeling*. Retrived from https://books.google.com.my.

Xiao, J.-D., Qiu, L.-G., Jiang, X., Zhu, Y.-J., Ye, S., & Jiang, X. (2013). Magnetic porous carbons with high adsorption capacity synthesized by a microwave-enhanced high temperature ionothermal method from a Fe-based metal-organic framework. *Carbon, 59*, 372–382. https://doi.10.1016/j.carbon.2013.03.032

Xu, R., Xiao, S., Yuan, J., & Zhao, A. (2011). Adsorption of methyl violet from aqueous solutions by the biochars derived from crop residues. *Bioresource Technology, 102*(22), 10293–10298. https://doi.10.1016/j.biortech.2011.08.089

Xu, Y., & Chen, B. (2013). Investigation of thermodynamic parameters in the pyrolysis conversion of biomass and manure to biochars using thermogravimetric analysis. *Bioresource Technology*, *146*, 485–493. https://doi:10.1016/j.biortech.2013.07.086

Yang, Y., Lin, X., Wei, B., Zhao, Y., Wang, J., (2013). Evaluation of adsorption potential of bamboo biochar for metal-complex dye: equilibrium, kinetics and artificial neural network modeling. *Int. J. Environ. Sci. Technol. 2,* 65(9), 234-251. https://dx.doi.org/ 10.1007/s13762-013-0306-0.

Yang, N., Zhu, S., Zhang, D., & Xu, S. (2008). Synthesis and properties of magnetic Fe_3O_4 -activated carbon nanocomposite particles for dye removal, *62*, 645–647. https://doi.org/10.1016/j.matlet.2007.06.049

Yakout, S. M., & Sharaf El-Deen, G. (2016). Characterization of activated carbon prepared by phosphoric acid activation of olive stones. *Arabian Journal of Chemistry, 9*, S1155–S1162. https://doi.10.1016/j.arabjc.2011.12.002

Yusof, Y., Yahya, S. A., & Adam, A. (2015). Novel technology for sustainable pineapple leaf fibers productions. *Procedia CIRP, 26*, 756–760. https://doi.org/10.1016/j.procir.2014.07.160

Zargar, B., Parham, H., & Hatamie, A. (2009). Fast removal and recovery of amaranth by modified iron oxide magnetic nanoparticles. *Chemosphere, 76*(4), 554–557. https://doi.10.1016/j.chemosphere.2009.02.065

Zimmerman, A. R., Gao, B., & Ahn, M.-Y. (2011). Positive and negative carbon mineralization priming effects among a variety of biochar-amended soils. *Soil Biology and Biochemistry, 43*(6), 1169–1179. https://doi.10.1016/j.soilbio.2011.02.005

Zhu, H.Y., Fu, Y.Q., Jiang, R., Jiang, J.H., Xiao, L., Zeng, G.M., … Wang, Y. (2011). Adsorption removal of congo red onto magnetic cellulose/Fe3O4/activated carbon composite: Equilibrium, kinetic and thermodynamic studies. *Chemical Engineering Journal, 173*(2), 494–502. https://doi.10.1016/j.cej.2011.08.020

Zhou, L., Shao, Y., Liu, J., Ye, Z., Zhang, H., Ma, J., … Li, Y. (2014). Preparation and Characterization of Magnetic Porous Carbon Microspheres for Removal of Methylene Blue by a Heterogeneous Fenton Reaction. *ACS Applied Materials & Interfaces, 6*(10), 7275–7285. https://doi.10.1021/am500576p

IR Frequencies

Characteristic IR Absorption Frequencies of Organic Functional Groups

Functional Group	Type of Vibration	Characteristic Absorptions (cm-1)	Intensity
Alcohol			
O-H	(stretch, H-bonded)	3200-3600	strong, broad
O-H	(stretch, free)	3500-3700	strong, sharp
C-O	(stretch)	1050-1150	strong
Alkane			
C-H	stretch	2850-3000	strong
-C-H	bending	1350-1480	variable
Alkene			
=C-H	stretch	3010-3100	medium
=C-H	bending	675-1000	strong
C=C	stretch	1620-1680	variable
Alkyl Halide			
C-F	stretch	1000-1400	strong
C-Cl	stretch	600-800	strong
C-Br	stretch	500-600	strong
C-I	stretch	500	strong
Alkyne			
C-H	stretch	3300	strong,sharp
-C≡C-	stretch	2100-2260	variable, not present in symmetrical alkynes
Amine			
N-H	stretch	3300-3500	medium (primary amines have two bands; secondary have one band, often very weak)
C-N	stretch	1080-1360	medium-weak
N-H	bending	1600	medium
Aromatic			
C-H	stretch	3000-3100	medium
C=C	stretch	1400-1600	medium-weak, multiple bands
Analysis of C-H out-of-plane bending can often distinguish substitution patterns			
Carbonyl	Detailed Information on Carbonyl IR		
C=O	stretch	1670-1820	strong
(conjugation moves absorptions to lower wave numbers)			
Ether			
C-O	stretch	1000-1300 (1070-1150)	strong
Nitrile			
CN	stretch	2210-2260	medium
Nitro			
N-O	stretch	1515-1560 & 1345-1385	strong, two bands

IR Absorption Frequencies of Functional Groups Containing a Carbonyl (C=O)

Functional Group	Type of Vibration	Characteristic Absorptions (cm-1)	Intensity
Carbonyl			
C=O	stretch	1670-1820	strong
(conjugation moves absorptions to lower wave numbers)			
Acid			
C=O	stretch	1700-1725	strong
O-H	stretch	2500-3300	strong, very broad
C-O	stretch	1210-1320	strong
Aldehyde			
C=O	stretch	1740-1720	strong
=C-H	stretch	2820-2850 & 2720-2750	medium, two peaks
Amide			
C=O	stretch	1640-1690	strong
N-H	stretch	3100-3500	unsubstituted have two bands
N-H	bending	1550-1640	
Anhydride			
C=O	stretch	1800-1830 & 1740-1775	two bands
Ester			
C=O	stretch	1735-1750	strong
C-O	stretch	1000-1300	two bands or more
Ketone			
acyclic	stretch	1705-1725	strong
cyclic	stretch	3-membered - 1850 4-membered - 1780 5-membered - 1745 6-membered - 1715 7-membered - 1705	strong
α,β-unsaturated	stretch	1665-1685	strong
aryl ketone	stretch	1680-1700	strong

MB removal by AC at different time interval.

10 min	20 min	30 min	40 min	50 min	60 min
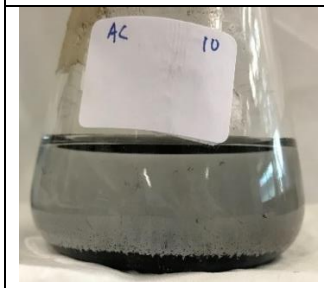	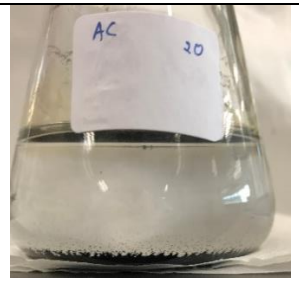		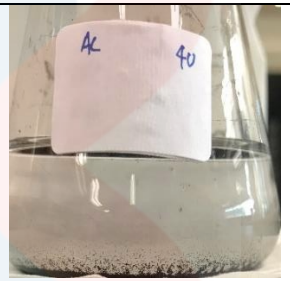		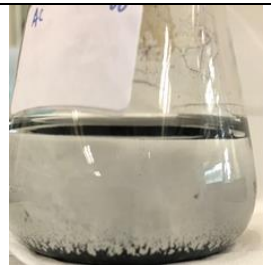

MB removal by MAC at different time interval.

10 min	20 min	30 min	40 min	50 min	60 min
	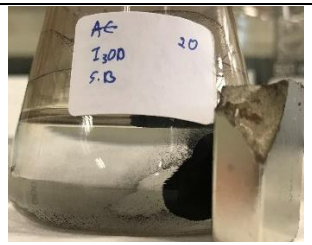	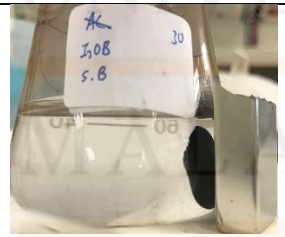	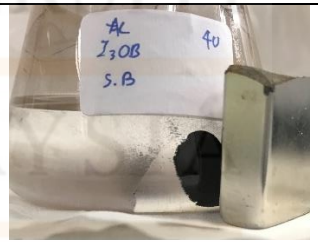	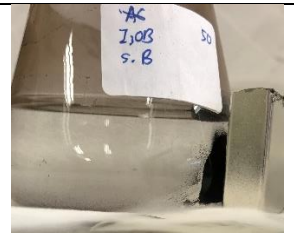	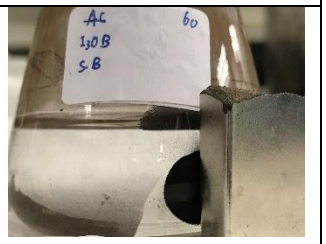

MB removal by MAC-CTAB at different time interval.

10 min	20 min	30 min	40 min	50 min	60 min
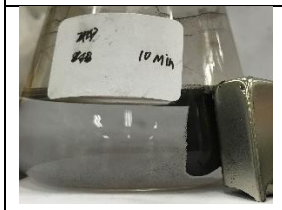	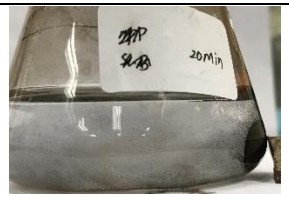	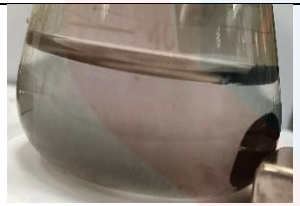	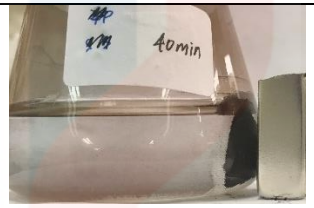	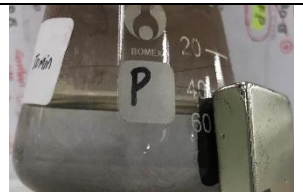	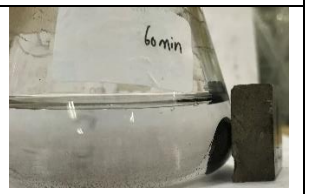

MB removal by MAC-CTAB at different time interval.

10 min	20 min	30 min	40 min	50 min	60 min
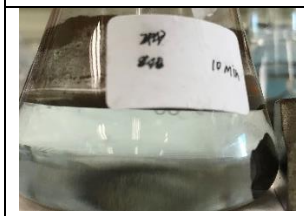	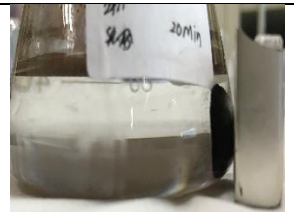	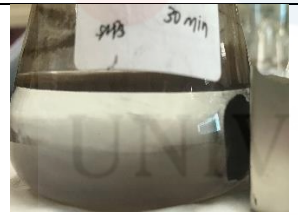			

MB removal by pMAC at different time interval.

10 min	20 min	30 min	40 min	50 min	60 min
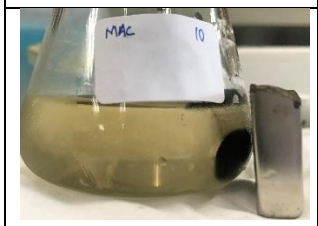	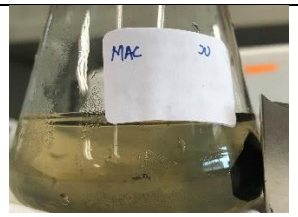	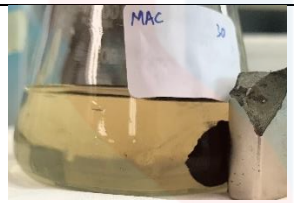	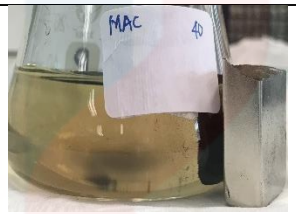		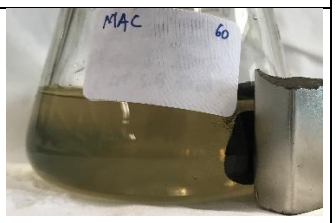

Visual Demonstration of Methylene Blue Removal